THE PROTON STOPPING CROSS SECTION OF GASES AT LOW ENERGIES

Thesis by

Harlan Kendall Reynolds

In Partial Fulfillment of the Requirements

for the Degree of

Doctor of Philosophy

California Institute of Technology

Pasadena, California

1953

ACKNOWLEDGMENTS

The experiment reported in this thesis is the joint work of several people. Those who have participated in all phases of the experiment are Doctors Ward Whaling, William A. Wenzel and D. N. F. Dunbar. Without their help the experiment would not have been performed and this thesis could not have been written.

Many helpful discussions were held with Professor R. F. Christy during the course of the experiment for which I am grateful. I wish also to thank the Office of Naval Research and Professors C. C. Lauritsen and W. A. Fowler for the opportunity to use the facilities of Kellogg Radiation Laboratory, and for a research assistantship this past year.

I also wish to thank my wife, Norma, for her constant faith and encouragement at all times and for her concrete help in the writing and typing of this thesis.

ABSTRACT

Proton stopping cross sections for gases and vapors were measured in the energy range 30 to 600 kev. A beam of protons was passed through a chamber with thin aluminum end walls containing the gas or vapor to be measured. The energy of the beam was measured before and after passing through the chamber and with and without the gas in the beam in order to measure the energy loss in the foils and in the gas. The beam was accelerated by an electrostatic generator, and the beam energies measured by an electrostatic analyzer and magnetic spectrometer.

The substances measured were air, H_2, He, N_2, O_2, Ne, A, Kr, Xe, H_2O, CO_2, CH_4, C_2H_2, C_2H_4, C_6H_6, NH_3, NO, and N_2O. Bragg's rule was tested by comparison of NH_3 with $N_2/2 + 3H_2/2$, NO with $N_2/2 + O_2/2$ etc., for H_2O, NH_3, NO, and N_2O, and found to be valid above 150 kev, except for NO. On the assumption of Bragg's rule, the stopping cross section of carbon was calculated from the data on the hydrocarbons, CO_2, and oxygen and hydrogen. The results were consistent for energies above 100 kev. The mean excitation potentials calculated from the measured stopping cross sections are: Oxygen, $I = 103 \pm 5$ ev; nitrogen, $I = 89.5 \pm 4$ ev; carbon, $I = 72.4 \pm 3$ ev; and helium, $I = 32.8 \pm 1.5$ ev.

TABLE OF CONTENTS

Section	Title	Page
I	Introduction	1
II	Theory	7
III	Experimental Method	12
IV	Results	27
V	Errors	35
VI	Straggling	43
VII	Tables I - VI	45
VIII	Figures 1 - 31	51
IX	References	84

I INTRODUCTION

In the measurement of cross sections for nuclear reactions, an important quantity entering the measurement is the amount of material being traversed by the beam in the case of thin targets, and the rate at which the bombarding particles are losing energy in the case of thick targets. In many experiments the overall accuracy is limited by insufficient knowledge of these quantities.

For a thin target of thickness dx, the cross section is defined as:

$$\sigma = \frac{Y}{N\,dx}$$

where Y is the yield in number of particles (or quanta) per incident particle (or quanta); N is the volume density of target nuclei; dx is a very small distance, of the order of 10^{-6} cm, and usually very difficult to measure. It is usually possible to measure ΔE, the average energy lost in the target. Then the cross section can be calculated from:

$$\sigma = \frac{Y}{N}\,\frac{dE}{dx}\,\frac{1}{\Delta E}$$

if $\frac{dE}{dx}$ is known. For a thick target the yield is the integral of many thin target yields, and the cross section can be written:

$$\sigma = \frac{1}{N}\,\frac{dE}{dx}\,\frac{dY}{dE}$$

and again involves the rate of energy loss, $\frac{dE}{dx}$.

The rate of energy loss is important in yet another technique first described by Snyder, Rubin, Fowler and Lauritsen[1].

This method uses thick targets and a magnetic spectrometer whose energy resolution picks out particles of a small range of energies which have come from a thin layer in the target. The formula for the cross section given by Snyder et al for cross section measurements of this kind is directly dependent on the rate of energy loss in the target material for the incoming and outgoing particle.*

The results of the present experiment and the discussions which follow are expressed in terms of the stopping cross section per atom (molecule) which is defined as:

$$\epsilon = \frac{1}{N} \frac{dE}{dx}$$

where ϵ is the symbol used for the stopping cross section; dE is the average energy loss in a small distance dx; and N is the number of atoms (molecules) per cubic centimeter. In the older literature on penetration phenomena, results are often quoted in terms of the stopping power. This is sometimes misleading since there are two different stopping powers, the differential and the integral stopping power; and the distinction between these two is sometimes confused. The differential stopping power at an energy E is defined as the ratio:

$$S = \frac{\epsilon(E)}{\epsilon_{air}(E)}$$

whereas the integrated stopping power S(E) is defined as the

---

*This last technique can also be used in reverse, that is, if the reaction cross section is known, the stopping cross section can be calculated from the observed yield. This is the method used by Wenzel and Whaling[2] to measure the stopping cross section of D_2O ice.

reciprocal of the average of $\frac{1}{s}$ averaged over all energies below a given initial energy, E. Or equivalently S can be defined as the ratio of the range in any substance divided by the range in air, corrected for the difference in atomic densities. s and S are equal only if s is independent of energy, which is not true for any substance, especially at the energies of this experiment. The two quantities do, however, become more nearly equal as the energy increases.

As well as for their interest in connection with nuclear reactions, stopping cross sections are of interest for their own sake, for the light they shed on collision phenomena. Especially in the energy range of this experiment, the known theory is sketchy and needs a solid experimental basis for further work. Bragg's rule is one theoretical concept which needs more experimental verification to find the limits of its applicability. Platzman[3] and Gray[4], in review articles on penetration phenomena, discuss extensively the validity of Bragg's rule, which states that the stopping cross section of a molecule is equal to the sum of the stopping cross sections of its constituent atoms. Bragg's rule, if valid, is an important and useful relation, and as stated above, implies independence of physical state. It, therefore, is not exactly true, since the stopping cross section is influenced by the quantum mechanical state of the electron, which is certainly not the same for valence electrons in molecules as in free atoms. Neither can these electronic states be completely independent of the physical state of the substance.

Platzman[3] and Gray[4] have both made estimates of the effects of association of atoms into molecules and conclude that at sufficiently high energies (higher in general than the range of the present experiment) they are small, about 1% of the total. Kramers[5] investigated the effects of conduction electrons in the metals and finds effects larger than 1%; but for effects in solids, other than metals, theoretical information is very meager, and the experimental information conflicting.

Stopping cross sections are also important to biophysicists engaged in investigations of radiation effects in living tissue. Water is the principal compound of interest in this connection, and the experimental data on water is particularly conflicting. Alpha particle ranges in liquid water have been measured by Michl[6] and Phillips[7] and the results are 12% lower than measurements by Phillips of ranges in water vapor, corrected for the difference in density, and 16 to 20% lower than calculations, based on modern data for water vapor, by Platzman[3]. Appleyard[8] measured the differential stopping power of liquid water for 4.5 Mev alpha particles, and finds a value 15% higher than Platzman's calculations and thus substantially in agreement with the results of Michl and Phillips. On the other hand de Carvalho and Yagoda[9] have measured alpha particle ranges in liquid water, water vapor, and ice and find agreement for the ranges in all three phases within 1%, and reasonable agreement with Platzman's calculations. Thus it is seen that the validity of Bragg's rule, when considering two different phases, is in doubt.

de Carvalho and Yagoda[9] offer the following explanation:

1. Michl's work[6] gave ranges which were too short because of poor emulsion sensitivity. In addition, there is some evidence, not as reproducible, of ranges of 38 microns, which are in agreement with the results of de Carvalho and Yagoda.

2. The two experiments by Phillips[7] and Appleyard[8] both involved detectors not in the water. Therefore, the alpha particles had to pass through an air-water interface where conditions might be anomalous in electron density. Also there arises the possibility of inadequate correction for the energy loss in air and in the detector window. Phillips used a visual scintillation detector; Appleyard, a thin window Geiger counter; and Michl and de Carvalho and Yagoda immersed photographic plates. This explanation seems to be possible, but the discrepancy seems very large to be accounted for in this way.

Water vapor is measured in this experiment over the same region as the measurements of Wenzel and Whaling[2] on D_2O ice. The two measurements do not agree; the measurements of Wenzel and Whaling give a stopping cross section 5 to 14% lower than the present experiment. This discrepancy is in the opposite direction from the early measurements, which gave a shorter range (higher stopping power and cross section) for liquid water than for water vapor, but in the same direction as the difference found with Kramers' results[5] for metals. The experimental situation then is still very much unresolved until the discrepancies are explained, either theoretically or as experimental errors.

Gray[4] discusses the applicability of Bragg's rule to gases and vapors and concludes that it is valid within 2%. He reports a few measurements contradicting this statement but feels they are due to experimental difficulties or errors. The present experiment shows that for the gases measured, Bragg's rule is valid above proton energies of approximately 150 kev, but invalid below this energy. There is one exception to this finding which will be discussed in Section IV.

Crenshaw[10], by a method similar to the present experiment, measured the rate of energy loss of charged particles in several gases, including air. However, his results are rendered doubtful by the fact that ranges calculated from his results for air do not agree with the ranges given by Bethe[11], which were determined from various range measurements and interpolated by a semi-empirical method. Thus the energy loss measurements have not been in agreement with range measurements; and the accuracy of neither was outstanding, especially in the low energy region where the simple theory does not apply.

This experiment was undertaken to resolve these discrepancies and to provide measurements of the stopping cross sections for the low energy region of as many light elements as are available in gaseous form. It was also proposed to measure several compounds in order to test Bragg's rule, and to measure the noble gases because of their interest for the future development of the theory of penetration phenomena.

II THEORY

Charged particles passing through matter lose energy by several processes, the most important process being loss of energy in collisions with electrons. However, at very low energies the particles also lose appreciable energy in collisions with atomic nuclei and in the process of capturing and losing of electrons. Capture and loss cross sections of electrons by protons have been measured experimentally in air by Kanner[12] and in hydrogen by Montague[13] and Ribe[14]. The effects of capture and loss can become important only when the capture cross section is comparable to the loss cross section. The ratio of these two, $\frac{\sigma_a}{\sigma_c} \approx 10$ or greater, for energies above 125 kev in hydrogen. The results are similar in air, being approximately independent of substance. This means positive ions will remain positive ions at energies above 125 kev.

The capture cross section is a very rapidly decreasing function of the energy, so that capture and loss phenomena are only appreciable below 200 kev for hydrogen, and 100 to 150 kev in other substances. The capture and loss contribution to the stopping cross section has not been investigated in any detail theoretically, but two types of contributions have been discussed in the literature.

While neutralized, the penetrating particle may have a different stopping cross section. This effect has been estimated by Warshaw[15], who concludes that the neutral stopping cross section

is approximately 1/2 that of a charged particle. In the process of capturing and then losing an electron, the heavy penetrating particle experiences a net loss of energy. If we assume the electron returns to the same state it started from, this loss would equal the energy gained by the electron in being given a velocity equal to the proton i.e. $1/2\ mv^2$, where m is the electron mass and v the velocity of the proton. However, the electron will not in general return to the same state, so there will be an additional loss of energy by the proton to remove the electron from its original state. Allison,[16] on the assumption that the average energy lost per capture and loss cycle is the same as the average energy loss per ion pair found at higher energies (35 ev), finds that the contribution to the stopping cross section in hydrogen is approximately 20% of the total at 50 kev and less than 1% at 175 kev. He finds similar contribution in air. Neither of these calculations appears to be too reliable; but they do serve to indicate that at these energies, capture and loss phenomena cannot be ignored in any theoretical treatment.

The leading term in most analyses, classical and quantum-mechanical, of the energy loss by collisions is inversely proportional to the mass of the struck particles and directly proportional to the charge squared. Thus, except for small corrections, the ratio of nuclear energy losses to electronic energy losses is:

$$\frac{m}{Z}\ \frac{Z^2}{MA}$$

where m is the mass of the electron; M is the mass of the proton; Z is the atomic number; and A the mass number of the struck atom.

This is approximately 1/3600 for most light elements in the energy range of this experiment. Below 25 kev proton energy, nuclear collisions do become important.

Bethe[17] using Born's approximation has shown that the stopping cross section per atom for protons is:

$$(II\text{-}1) \qquad \epsilon = -\frac{1}{N}\frac{dE}{dx} = 2\kappa Z \ln \frac{2mv^2}{I}$$

where $K = \frac{2\pi e^4}{mv^2}$ and is the leading term mentioned above; Z is the atomic number of the atoms; e is the electronic charge; m is the electronic mass; v is the velocity of the penetrating particle; and I is the mean excitation energy of the electrons in the atom, and is defined as:

$$(II\text{-}2) \qquad \ln I = \sum_n f_n \ln \varepsilon_n$$

where f_n is the effective oscillator strength, and ε_n is the effective excitation energy of each electron, when the atom is considered as an assembly of oscillators. Formula (II-1) is valid for non-relativistic energies for which $E >> \frac{M}{m}\varepsilon_n$ for all electrons in the atom. E_n is the kinetic energy of an electron in the nth shell of the atom. This condition is a very restrictive one which is frequently not fulfilled in the regions of experimental interest and is not fulfilled, for all energies, for any of the substances studied in this experiment. Livingston and Bethe[18], Brown[19], and Walske[20] have calculated more accurately the contribution of the K electrons and give as their result for the total stopping cross section:

$$(II\text{-}3) \quad \epsilon = 2KZ\left(\ln \frac{2mv^2}{I} - \frac{C_K}{Z}\right)$$

where C_k is a number of order 1 or less given in graphical form and as an asymptotic formula by Walske[20]. This formula is valid then for energies $E \gg \frac{M}{m} E_L, \frac{M}{m} E_M$ etc., which is less restrictive but still not fulfilled except at the highest energies and lightest elements of this experiment. In principle, the same correction can be given for the L-shell, etc.; but this has not been done because of the lack of knowledge of the proper wave functions for L-shell electrons.

Strictly speaking, the above formulae apply only to monatomic gases; but it is known that binding into molecules will not alter the stopping power very greatly. This is the whole question of the validity of Bragg's rule as applied to gases. Platzman[3] notes three possible effects when atoms are combined into molecules:

1. The values of I may be altered by changing of the excitation energies (E_n) and the oscillator strengths of the system.

2. & 3. The incident particles may excite rotational and vibrational modes of the molecule.

The latter two effects have been estimated by Platzman[3] to be:

$$\epsilon_{vib} \approx K\left(\frac{W_{vib}}{13.6\,ev}\right)\left(\frac{\mu}{\hbar^2/mc}\right) \ln \frac{2mv^2}{W_{vib}}$$

and

$$\epsilon_{rot} \approx K\left(\frac{W_{rot}}{13.6\,ev}\right)\left(\frac{\mu}{\hbar^2/mc}\right) \ln \frac{2mv^2}{W_{rot}}$$

where W_{vib} and W_{rot} are the first vibration and rotation energy levels, and μ is the dipole moment. These energy levels are quite

small compared to 13.6 ev, so that in spite of the logarithmic factor being increased, the contribution of these processes to the total stopping cross section is roughly 1%. However, it is possible the contribution is more appreciable near and below 100 kev for protons.

The first effect mentioned above is more difficult to calculate, since it is not even possible to calculate I for an atom with any accuracy, except for hydrogen. It is probable that the oscillator strengths of all electrons, which depend on the occupation density of the states higher than the one under consideration, are altered in a molecule since there is presumably a fuller occupation of the lowest discrete states in a molecule. The excitation energies, particularly of the outer electrons, are also changed, probably increased since they are more tightly bound in a molecule. These two effects are opposite in their effect on the stopping cross section, and therefore it is not possible to predict with any certainty their net effect without a detailed knowledge of the energy levels and oscillator strengths. Platzman[3] believes that I will usually be decreased, and ϵ therefore increased.

For solids and liquids, there is a possibility of other effects due to the close proximity of molecules to each other. The size of such effects is not known except for metals, where the effect of the conduction electrons has been studied by Kramers[5]. Additional discussion of possible effects in solids and liquids is given by Platzman[3].

III EXPERIMENTAL METHOD

The method used in this experiment is very simple and essentially involves the use of a beam of protons of known initial energy, passing through a gas chamber, whose end walls are very thin aluminum foils. The energy, after passing through the chamber, is measured, first without gas in the chamber, then with gas present. The energy loss in the foils and gas can then be calculated in a simple way, and the amount of gas determined from temperature and pressure measurements.

The simplest, most straightforward, way to make the measurements is to fix the energy of the entering particles and measure the different energies of the particles emerging from the gas chamber under the various conditions. In this experiment, however, the energy of the emerging particles is kept fixed, and the entering energy changed to enable the particles to emerge with the proper energy.

The reasons for this method are several. In the first place, the energy of the emerging particles is determined by a magnetic spectrometer. It is possible to measure the energy by measuring the magnetic field; but the easiest way to use a magnetic spectrometer is simply to regulate the current of the magnet to a constant value, and change the incoming energy to the gas chamber. This incoming energy is easily measured by an electrostatic analyzer, which is part of the accelerator. This eliminates the need for a magnetometer. Of course, the magnetic field is not always the same for each current setting, but all that is required is that it remain constant during

one energy loss determination. This requirement is met by the current regulator, whose regulation characteristics are not known; but the constancy of the field is checked by measuring the foil profile, both before and after the foils-plus-gas profile (see discussion later in this section for details of method).

The second reason for the somewhat backward method is to improve the shape of the spectrum of particles observed by the detector. The spectrum observed, if the magnetic field is held fixed and the bombarding energy varied, has a sharp leading edge and a flat top. The leading edge is at the lowest energy at which particles can be scattered from the gold and have the proper energy to reach the detector at the spectrometer output. Then as the energy of bombardment is increased, particles are scattered from deeper layers in the gold and lose energy before reaching the spectrometer, so that some of them still have the proper energy to reach the detector. These particles were scattered when they had a higher energy than the particles corresponding to the leading edge. The spectrum then has a nearly flat top, which decreases with increasing energy approximately as the reciprocal of the energy squared, since the scattering cross section decreases in this manner. This decrease in the height of the spectrum is approximately compensated for by the fact that particles are lost by scattering in the foils and gas. This loss again decreases approximately as the reciprocal of the energy squared. The fold of these two functions is a step function with quite a flat top, which is what is actually found in the experiment (see fig. 2).

The third reason for keeping the magnet fixed is that it is much easier to vary the beam energy than the magnet.

The beam of protons or deuterons is accelerated by a 600 kev electrostatic generator. The energy is determined and kept constant by an electrostatic analyzer. This equipment has been described by Wenzel[21]. The beam is collimated before striking the target by passing through a hole .020 inch in diameter. The schematic diagram of the most important features of the apparatus is shown in figure 1.

The gold target is set at a 45 degree angle to the incoming beam and to the spectrometer. The particles are scattered elastically from the gold, so that those scattered at 90 degrees into the gas chamber have an energy $\frac{A-1}{A+1}E$, where A is the atomic mass number of gold and E is the energy of the particles before scattering ($\frac{A-2}{A+2}E$ for deuterons).

Between the scattered beam and the spectrometer is the gas chamber, which can be moved out of the scattered beam when desired. The gas chamber is 2.886 inches in length; the aluminum foils are .093 inch in diameter; and over the foils is placed a tantalum sheet with a hole of .045 inch in diameter to allow the particles to go through the center portion of the foils only. The pressure in the gas chamber is measured by an oil manometer, using Litton oil, whose density was measured to be $0.886 \pm .001$ gm/cm^3. The temperature was measured by a mercury thermometer placed in a small oil cup, bolted to the top of the target chamber.

After passing through the gas chamber, the particles enter a 16-inch radius magnetic spectrometer, and are detected by a zinc sulphide screen scintillation counter. The magnetic spectrometer is more fully described by Li[22].

As noted previously, the spectrum of particle energies, entering the spectrometer, is essentially a flat-topped step function. The leading edge of this spectrum has a slope determined by the energy resolution of the spectrometer, (approximately 1%) and the straggling in the foils and gas. The half-height point on this steep portion, when the gas chamber is moved out of the way of the beam, is taken to be the energy to which the magnet is set. The magnet is then held constant, and the foils are placed in the beam. An increased energy of bombardment is now necessary, and the spectrum is displaced to higher energies. This displacement is measured to the half-height point of the new spectrum. Similarly, there is a further displacement when a gas is introduced into the gas chamber.

Let us denote by E_o the energy as measured above without foils; by E_f that measured with foils in the beam; and by E_g that measured with gas in the chamber. Then:

$$E_f - E_o = \Delta F_1 + \Delta F_2 \qquad \text{(III-1)}$$

where ΔF_1 and ΔF_2 are the energies lost in the first and second foils respectively.

$$E_g - E_o = \Delta F_1' + \Delta F_2' + \Delta E_g \qquad \text{(III-2)}$$

where ΔE_g = energy lost in gas and $\Delta F_1' \neq \Delta F_1$.

But $\Delta F_2 = \Delta F_2'$. Since the final energy of the particles emerging from foil 2 is always the same, the energy entering foil 2 is the same and therefore the loss. In foil 1, however, the average energy is not the same with and without gas in the chamber so that the energy loss, which is a function of energy, is different. Substituting (III-1) into (III-2):

$$(III\text{-}3) \quad E_g - E_o = \Delta E_g + E_f - E_o + (\Delta F_1' - \Delta F_1), \text{or}$$

$$(III\text{-}4) \quad E_g - E_f = \Delta E_g + \frac{\partial(\Delta F_1)}{\partial E}(E_g - E_f) + \ldots$$

where $\frac{\partial(\Delta F)}{\partial E}$ is evaluated at $E = \frac{E_g - \frac{\Delta F_1'}{2} + E_f - \frac{\Delta F_1}{2}}{2}$

or $E = \frac{E_g + E_f - \Delta F_1}{2}$

This gives:

$$(III\text{-}5) \quad \Delta E_g = (E_g - E_f)\left(1 - \frac{\partial(\Delta F_1)}{\partial E}\right)$$

The two foils are made in such a way as to be equally thick so that $\Delta F_1 = \frac{E_f - E_o}{2}$. The correction term in equation (III-5), $\frac{\partial(\Delta F_1)}{\partial E}$, is $\leq 4\%$ for all energies and all foils used.

The effective energy of the measurement is taken to be the mid-energy between the energy entering the gas and that leaving it. This energy is:

$$(III\text{-}6) \quad \bar{E} = \frac{(E_g - \Delta F_1') + (E_o + \Delta F_2')}{2}$$

which is approximately $\bar{E} = \frac{E_g + E_o}{2}$, since $\Delta F_1'$ is nearly

equal to $\Delta F_2'$. The difference is negligible compared to $E_g + E_o$. The average energy loss over the above range of energies, $E_g - \Delta F_1'$ to $E_o + \Delta F_2'$, is then taken to be equal to the instantaneous rate of energy loss at the energy $\frac{E_g + E_o}{2}$. This assumption is true only for small energy losses. Warshaw[15] has calculated the error in this assumption on the assumption that the rate of energy loss is a linear function of the energy over a region ΔE. He finds that the stopping cross section at the energy $\bar{E}$ is:

$$\epsilon_{\bar{E}} = \frac{1}{N} \frac{\Delta E}{\Delta x} \left(1 + \frac{(\lambda \tau)^2}{12}\right) \qquad \text{(III-7)}$$

where λ is the slope of the ϵ curve in the region being measured, and τ is the number of atoms per cm^2 in the chamber. For CO_2 at 45 kev, one of the worst cases, $\lambda \tau \approx .2$ and the correction is only 1/3%. This correction was not applied to any gas.

There is an alternative graphical method of calculating the energy loss. A range-energy curve is made for aluminum, which need not be in any absolute units of range, nor absolute in range zero point. The curve must be drawn, however, so that energies and ranges can be read to at least three places. The graph used for the low energy calculations covered forty-four sheets of fine graph paper ($8\frac{1}{2}$ x 11 inches) for the energy range 13 to 295 kev.

The range at energies E_f and E_g are found on the graph; from each is subtracted the range in the foils. The result is the range of the particles leaving and entering the gas. The energies are found from the graph, and the difference is the energy loss in the gas. The effective energy of the energy loss is taken to be the mid-point of these two energies. This method automatically

takes account of the change in energy loss in the foils, since the thickness of the foils is subtracted in range units instead of energy units.

Most of the measurements for proton energies, less than 125 kev, were actually made with deuterons as the bombarding particles. As shown in Section II, the stopping cross section is a function of the velocity and charge of the bombarding particle only. Therefore, a deuteron of energy E is equivalent in rate of energy loss to a proton of energy E/2. In the region of 125 kev, equivalent proton energy measurements were made using both protons and deuterons; and no differences in results were found. The use of deuterons is very useful because it allows the electrostatic generator to be operated at a higher voltage where it is more stable and gives a larger beam of particles. Also the scattering in the foils and gas, which causes a loss of particles, is a function of the energy only and is less at the higher energies of deuterons. Finally, the scintillation detector used on the spectrometer rapidly loses sensitivity at the lowest energies. Using deuterons makes measurements possible at lower energies than the use of protons would. The benefits of a higher generator voltage are increased further by the use of diatomic (HH^+) ion beams for the energy range 300 to 125 kev and diatomic (DD^+) deuteron beams below 125 kev. Thus for points of equivalent proton energy of 25 kev, the generator is actually operating at 100 kev.

Experiments were performed to measure the effects of any of four possible systematic errors. The first two are stretching of the foils under pressure by the gas and adsorption of the gas in

the foils. The first will tend to give a falsely low value of the energy loss in the gas, since the energy loss in the aluminum will be less when the gas is present. The second possibility will have the opposite effect since there will be more gas present than indicated by the pressure and temperature readings. The net effect of these two phenomena can be tested by making the chamber very short, so that there is a very small amount of gas present; but the stretching and adsorption will still be as large as before. Such a short chamber was made with a gas path length of .040 inch which should give an energy loss in the gas of 1.4% of that obtained in the normal length cell for the same pressure and temperature. Measurements were made on N_2, C_6H_6, O_2, H_2O, and NH_3. The ratios of the displacements found, to those expected from the known gas path, varied from 1.3 for N_2 and H_2O, to 0.3 for O_2 and NH_3, with the ratio for C_6H_6 being 0.75. The accuracy of these ratios is about 50% so that it is concluded that the net effect is $0.0 \pm 1\%$.

Two other possible sources of systematic error are connected with the scattering of the beam. Large angle nuclear scattering and multiple scattering are proportional to the reciprocal of the energy^2 and to Z^2. For heavy elements at low energies, there is a very large attenuation of the beam, both in passing through the foils and the gas, because of the very restricted geometry of this experiment. The angle subtended at one foil by the hole in the other foil is only .89 degrees. The question arises as to whether or not those particles lost by scattering were on the average losing energy at a different rate than those not scattered and

whether or not any appreciable number will be scattered back into the usable solid angle and change the average energy of those counted. These questions were investigated experimentally in two ways.

Particles are scattered out of the beam in the foils as well as in the gas. But in order for scattered particles to enter the spectrometer on a path which will reach the counter, they must be scattered at least once in the gas or from the wall of the chamber. The number of particles scattered in the gas will increase if the pressure is increased and other conditions remain the same. They will have travelled a longer path than is assumed in the calculation of ϵ and therefore will increase the measured ϵ. This increase will increase with pressure. Experiments to find this effect, if it exists, were performed on several gases. Particular attention was paid to krypton and xenon at low energies, where it was expected that the effect would be a maximum.

With the spectrometer magnet kept constant, the energy loss was measured at several different pressures. For krypton, data was taken at two pressures for each of two magnet settings, for proton energies of approximately 50 and 77 kev. In one case with 6.16 cm of oil pressure, the result was a 2.5% higher stopping cross section than with 3.08 cm oil pressure. This difference is corrected slightly to account for the small change in average energy in the gas. In the other case, the higher pressure (8.12 cm oil) gave a 1% higher cross section than the point at 2.00 cm oil pressure. This might indicate a small pressure dependence.

But it must be remembered that the accuracy of any individual point is of the same order as the above differences. For xenon, measurements were made at one magnet setting for five pressures--- 8.13, 5.95, 4.07, 2.00, and 2.04 cm oil. The scattering of the points was large, approximately 3% from the highest to the lowest cross section; and no trend with pressure was discernible. Similar measurements were also made on air and N_2O, and no discernible trend with pressure was found. There is no pressure effect that is as large as the experimental error of this experiment.

The effects of scattering from the wall were reduced by lining the walls with aluminum, which has a lower Z than brass. The effects of scattering in the gas were reduced by putting four thin aluminum baffles, spaced through the chamber. These baffles reduced the aperture through which the particles must go to 3/16 inch from the chamber diameter of 3/8 inch. (See fig. 1) Data was taken on several gases, notably air and oxygen both with and without these baffles; and no difference in result was observed. Measurements over the full energy range 30 to 600 kev were taken on argon with the hole in these aluminum baffles further reduced to 1/8 inch. The loss of particles was 20% to 30% greater than the previous loss, but no difference in stopping cross section was found.

If scattered particles suffer on the average more energy loss than non-scattered particles, then it would be expected that any increase in effective solid angle would increase the measured energy loss. Such an increase of solid angle was effected by

increasing the size of the second aluminum window to 3/16 inch and removing the tantalum exit baffle. Measurements of the stopping cross section of air at 130 kev and 500 kev made with this larger foil, did not differ from those made with the small foils within the experimental error. This measurement was made with no aluminum baffles inside the gas chamber.

It has been found in experiments with charged particle beams in a vacuum that a deposit of carbon tends to build up upon any surface which the beam strikes. If such a deposit is on the surface of the gold scatterer, it will cause an additional loss of energy by the particles. This additional energy loss, if it doesn't change with time, will cause an error in the energy scale, since it will then be uncertain as to what the energy of the particles was after scattering. Since the deposit is thin, this is usually unimportant. However, if it changes in the course of an energy loss measurement, it may cause a more important error.

The depositing of carbon, which apparently comes from vacuum pump oil vapor, is reduced by placing a liquid air cold trap in the vacuum system between the pump and the gold target. To see that no significant amount of carbon is deposited during a measurement, E_f is measured both before and after measuring E_g. Usually the measurement is the same. If not, the average of the two is taken, and the target is moved to present a fresh surface to the beam. Measurements taken in this way and measurements taken with no observed carbon deposit did not show any systematic difference.

This practice of measuring E_f twice for each measurement provides a check on the constancy of the magnetic field. Occasionally the measurement of E_f indicated a change which was in the wrong direction to have been caused by a carbon deposit. These changes were ascribed to changes in the magnetic field and were never greater than 2% of the energy loss. The average of the two measurements was taken as the value of E_f.

Another important possible systematic error, which must be investigated, is contamination of the desired gas with unknown gases. Table I shows the manufacturers' purity claim and the manufacturer for each gas used, and the principal impurity where known. The standard purifying method used for this experiment was passing the gas through Drierite (anhydrous $CaSO_4$) before using, which removes any water present. Unless otherwise stated, this was the only method used. The gas container was connected to a tube containing the Drierite, which was in turn connected to the chamber by a valve; the tube was flushed several times to remove the air. Contaminating gas present from the start in the Drierite tube (principally air) will be diluted during use. Measurements were taken in such a way that any systematic change in ϵ caused by such a contamination would show up as a systematic difference between neighboring points on the curve. No such effect was observed. Continuously added contamination was avoided by having the gas being measured at a higher pressure than atmospheric whenever possible.

The liquids, H_2O, C_6H_6, were purified and air removed by freezing with liquid air, pumping off unfrozen gases, melting and

repeating this process several times. Krypton, neon, and xenon were received in sealed glass flasks and were not further purified. Hydrogen was measured after purification by two methods. The first method was to dry with Drierite as in the standard method outlined above, and in the second the hydrogen was passed through a Palladium leak. No significant difference between the two methods was found. NO and C_2H_2 were passed through a dry ice and alcohol cold trap. The cold trap removed NO_2 and N_2O_3 contaminants from NO and removed from the C_2H_2 the acetone in which C_2H_2 is normally dissolved for shipment.

The fact that hydrogen shows no difference in measurements for the two purifying methods is a good check that, with care, little contamination results from connecting the gas to the gas cell. Hydrogen should be quite sensitive to any contamination of air since its stopping power is so low compared to air.

An important factor in the success of the experiment was the making of foils thin enough to have a low energy loss in the foils, but thick enough to hold a pressure which would give sufficient energy loss in the gas. Aluminum foils to fit these requirements were made by a process suggested by workers at Los Alamos[23]. They were made 30 to 65 μ gm/cm^2 in thickness. The energy losses in the foils were thus 4 to 20 kev per foil, and held pressures as high as 25 cm of oil (10 mm of Hg) with no measurable leaking.

The foils are made by floating a drop of zapon on a water surface. The zapon solidifies to a thin flexible film, which is picked up from the water on the foil holder. The zapon is dried

and aluminum is evaporated onto the film in a vacuum. The proper thickness of aluminum is judged by viewing the filament, from which the aluminum is evaporated, through the zapon-aluminum film. If evaporation is continued until the glowing filament is just visible, the resulting thickness is approximately 50 μ gm/cm^2. One can make thin or thick films, judging the thickness by experience. The zapon film must be removed since it is quite thick in energy units. Attempts to burn off the zapon by passing the direct ion beam of the electrostatic generator through the foils were unsuccessful, because of a residue of carbon left on the aluminum, which made the films uneven in thickness. The method finally adopted for removing the zapon, was to place a drop of acetone on the zapon side of the zapon-aluminum film, which dissolves the zapon readily, and then quickly remove the acetone with absorbent paper.

The uniformity of the film is verified by the fact that the straggling is approximately what is to be expected from simple straggling theory discussed in Section VI. The shape of the energy loss curve in the aluminum agrees with that found by Warshaw[15]. It is concluded from this that the amount of zapon or other material left with the aluminum is small. These considerations are sufficient since the thickness of the foils and the shape of the foil energy loss curve are used principally as corrections to the gas energy loss, whose maximum size is 4%. The foil energy loss also affects the effective energy of the measurement $\bar{E}$ but is in general only a small fraction of $\bar{E}$. (See equations III-5 and III-6)

The two foils used at any one time are always made together at the same distance from the evaporating filament, and so are assumed to be equally thick. Measurements made with a simple photocell arrangement of their light transmission confirm their equality to a few per cent. The measured light transmission of the thinnest foils, successfully used, was approximately 50%.

IV RESULTS

The results of this experiment are presented in tabular form in Tables II through V and in graphical form in figures 3 through 31. Tables II and III give the adopted values of stopping cross sections taken from the original smooth curves. Tables IV and V give the values of the differential stopping power for each substance measured.

Figure 3 shows the results for the light elements which exist in gaseous form. Some of the features can be explained qualitatively. At high proton energy, ϵ(helium) is seen to be approximately twice as large as ϵ(hydrogen), as would be expected from the fact that helium has twice as many electrons as hydrogen. The helium cross section is not quite twice the hydrogen cross section, since helium has a higher mean excitation energy. As the energy decreases, the higher excitation energy in helium becomes progressively more important. At low enough energies, we see that this effect is so strong that helium has little more stopping cross section than hydrogen; that is, it has only one effective electron.

Similarly, oxygen has a higher first ionization potential (and, therefore, presumably higher mean excitation energy) than nitrogen; this would make ϵ(oxygen) lower than ϵ(nitrogen), as appears to take place at low energies. At high energies, the stopping cross section is determined more by the number of electrons than by the excitation energy; and, therefore, oxygen has a higher stopping cross section than nitrogen at energies above 150 kev.

It must be noted, however, that what is actually measured is the stopping cross section per molecule, which is divided by two and called the stopping cross section per atom. It is possible that the various molecular effects discussed in Section II are so strong at low energies (100 kev and lower) that they obscure such electronic effects mentioned above.

By the use of formula (II-3), it is possible to calculate the mean excitation potential from the measured stopping cross sections for oxygen, nitrogen, carbon, helium and hydrogen. This calculation is made somewhat uncertain for oxygen and nitrogen because of the limited energy range for which C_k has been calculated by Walske[20]. For oxygen it is necessary to make a questionable extrapolation of Walske's curve for C_k to calculate the mean excitation energy at 600 kev. It is impossible to make any calculations for oxygen at lower energies. For nitrogen, extrapolation is necessary at 550 kev and below. The results of this calculation for oxygen and nitrogen are $I = 103 \pm 5$ ev, and $I = 89.5 \pm 4$ ev, respectively. For carbon, calculations are possible without extrapolation to 400 kev; and the average I from calculations at five energies is $I = 72.4 \pm 3$ ev, which is in good agreement with the value of 74.4 ev found by Mather and Segrè[24] from measurements made at 340 Mev. The difference of these I's represents a difference in the stopping cross section of less than 1%, so the agreement is really remarkable. For helium, the average of six calculations over an energy range of 600 to 350 kev is $I = 32.8 \pm 1.5$ ev. Below 350 kev, the calculated I begins to decrease with decreasing energy. The probable error shown is that estimated from the error

of the stopping cross section.

As a step in the process of calculating the K-shell correction, the complete stopping cross section of a hydrogen atom is found. A formula for the hydrogen stopping cross section is given by Walske[20]; calculations from this formula are 6% to 31% lower than the values measured in this experiment, with the difference largest for the lowest energies calculated (300 kev). This may mean that these K-shell corrections can only be used when the correction is small, as it is for most elements. The correction to ϵ for oxygen at 600 kev is only 2%; to ϵ for nitrogen, 3.5%; to ϵ for carbon, 5%; and to ϵ for helium, 4%. The reason for the hydrogen discrepancy is not known; but regardless of the reason, it seems reasonable to continue to regard K-shell corrections as valid as long as they are small, which they are in the calculable range of energies.

Figures 4 and 5 show the results for a number of compounds, both gases and vapors, and also the stopping cross section to be expected from Bragg's rule. It is seen that, except for NO, Bragg's rule seems to hold quite well for energies above 150 kev, but not at all well below these energies. The reason for the discrepancy at all energies in the case of NO is not known. One's first suspicion is an admixture of NO_2. The experiment was done first purifying the gas by drying it with $CaSO_4$ drying agent. Then it was repeated with the gas piped through a trap cooled with a dry ice alcohol mixture. This removed a noticeable brown color (NO_2) but failed to change the measurement results by an appreciable amount.

This discrepancy in the case of NO is not entirely unexpected. Schmieder[25] found discrepancies for the three simplest oxides of nitrogen, but these are attributed by Gray[4] to experimental difficulties. Platzman[3] suggests the possibility of unusual features for molecules such as NO, and NO_2 which have an odd electron. These remarks certainly do not constitute an explanation.

Figure 4 also shows the results for D_2O ice as found by Wenzel and Whaling[2]. The discrepancy is obvious and unexplained and certainly may be real. The results of Wenzel and Whaling are supported by the agreement of their measurement of the $D(d,p)H^3$ cross section, based on their ϵ measurements, with other measurements by independent methods. The results of this experiment are supported by their agreement with Bragg's rule. The discrepancy is opposite to that found for liquid and water vapor (Platzman[3]).

The fact that Bragg's rule does not hold at all well at low energies can be qualitatively explained in the following way. At low energies the deeper electrons are so tightly bound it becomes more difficult for the proton to excite them, and thus the outside or valence electrons play an increasingly more important part in the stopping as the energy of the penetrating particle decreases. These valence electrons are, of course, in quite different states in different molecules; and so their individual stopping cross sections may vary considerably. Thus we would expect that 1/2 the molecular cross section of gases such as O_2 and N_2 may not be a reliable measure of the atomic cross section at low energies.

Figure 6 shows the results, including the experimental points, for four hydrocarbons. There were at least as many experimental points for each other gas and in several cases many more as shown in figures 15 through 31. If we assume the validity of Bragg's rule, we can subtract the measured stopping cross section contribution of hydrogen from these four hydrocarbons and thus get the carbon stopping cross section. This calculation has been made and the results are shown in figure 7. Here again we see that Bragg's rule seems valid above 150 kev; that is, we get reasonably consistent values for the stopping cross section of carbon; but below 150 kev the calculated stopping cross sections vary widely.

Among the four hydrocarbons, there are five independent pairs (only five because benzene is a multiple of acetylene) of gases which can be used to calculate by Bragg's rule the stopping cross sections for both carbon and hydrogen, independently of any measured value for hydrogen. Even if all the hydrocarbons are taken to be equally accurate percentagewise, the values of the stopping cross section for hydrogen and carbon derived from each pair have a different probable error, calculated in the usual way. This difference arises because of the different proportions of hydrogen and carbon in each compound. Those pairs for which the derived value for hydrogen is most accurate give the least accurate stopping cross section for carbon and vice versa. Hydrogen and carbon stopping cross sections have been calculated in the above way, and a weighted average taken, weighted according to the accuracy of the determination from each pair. The results of this calculation are shown by the dashed curves of figure 8.

The solid curve is, in the case of hydrogen, the experimentally measured one, and in the case of carbon, that derived by the first method mentioned. The good agreement simply means that the various measurements are consistent with each other, i.e. systematic errors, if any, are the same for all gases and no one gas has been subject to a peculiar systematic error. This is especially gratifying for hydrogen, since hydrogen and helium are the most difficult to measure and give the least accurate results.

Figure 9 gives the stopping cross section for air and includes the experimental points. This illustrates the scatter of the individual points when a great many points were taken. Air was used as a standard and was repeated at various times and under various conditions to check the reproducibility of the results. The results were always reproducible except for a group of high energy points taken early in the experiment which were systematically lower than all later results, which were repeated several times. These early results were not used in fixing the smooth curve and do not appear in figure 9.

Figure 10 gives the range of protons in air, the smooth curve being the range calculated by integrating the results of this experiment numerically and taking the range at 20 kev as that given by Bethe[11]. The dashed curve is from Bethe. The dots are the ranges measured by Bøggild[26], and by Hughes and Eggeler[27].

The range curve given by Bethe[11] is based upon the best previous experiments on ranges in air using both alpha-particles and protons. The lowest energy measurements for proton ranges are

those shown in figure 10. These range measurements are believed to be quite accurate and Bethe's range curve is fitted to them. The shape of the range curve is based upon the theoretical energy loss, formula (II-3), modified somewhat arbitrarily to fit the range measurements and to pass through the origin. It is not surprising that the shape of the range curve derived from this experiment is slightly different from that of Bethe, but the agreement within experimental error of the ranges with the cloud chamber measurements is an excellent check on systematic errors of this experiment and gives confidence to the belief that this experiment does not have very large systematic errors. The agreement probably cannot be improved by adjusting the range assumed at 20 kev, since almost any shape for the ϵ curve which meets the curve at 20 kev, will give approximately the same range as that assumed. The range at 20 kev is only a small fraction of the total range and cannot be changed greatly; so the error introduced by the assumption regarding the 20 kev range must be small, probably less than 1%.

In figure 12 is shown the results found in four different experiments for the stopping cross section of argon. The results of this experiment are seen to be in good agreement with those obtained at Ohio State[28] and Chicago[29], but there is a discrepancy of 10 to 12% with the results found in the experiment at Los Alamos[30]. A discrepancy in the same direction and of the same order of magnitude is found between the Los Alamos data and our data for Kr, N_2, O_2 and CO_2. This is well outside the experimental errors. Agreement with the Los Alamos data within experimental error (3%) is found for H_2, He and H_2O.

The experimenters at Chicago[29] also measured air and agreed equally as well with our data as in the case of argon. The Ohio State group[28] also measured N_2, neon, krypton and xenon in the energy region from 400 to 1000 kev, and in the region overlapping our data the agreement is good for N_2, and Ne. Our data for krypton is lower than theirs by approximately 4% and their data for xenon is lower than ours by 13%. The krypton difference is within experimental error, but the xenon difference is not. The most likely source of such a large discrepancy for a single gas is that the gas was contaminated; this would mean for heavy gases such as krypton and xenon that the measured stopping cross section would be lower for the contaminated gas.

In the course of this experiment many gases have been measured more than once over the same energy range. The results above 150 kev have been reproducible at all times for all gases except for the one group of five measurements of air which were mentioned previously. The situation below 150 kev is not so fortunate, as small systematic differences were found in the results for C_2H_2, O_2, N_2, and argon. These systematic differences were never large, varying from 2 to 5%. The adopted curve was drawn through the center of gravity of all measurements. Air and several other gases were measured several times, and no systematic differences were found. The reason for these differences found which were greater than the scatter of one group taken at one time are not known, so that it can only be concluded that the results of all gases are less certain below 150 kev than over the rest of the energy range of this experiment.

V ERRORS

The probable error of this experiment and its sources will be discussed under two headings, random errors and systematic errors. Random errors include those which in any group of measurements on one gas are randomly distributed. Systematic errors include those which are the same for all measurements of a given gas.

The largest single source of random error in the experiment is the determination from the observed spectra, of the energy loss in the gas. It arises principally because of the statistical nature of the data for the spectrum curves, because of small variations in the bombarding energy, and because of straggling in the foils and gas. It is estimated that the probable error of the determination of the mid-point of the spectrum is as follows:

Monatomic proton (H^+) ion beam	± 0.4 kev
Diatomic proton (HH^+) ion beam	± 0.3 kev
Diatomic deuteron (DD^+) ion beam	± 0.4 kev

There are of course two midpoints to be determined for each energy loss measurement, so that the probable error of the energy loss measurement is for each case given above ± 0.6 kev, ± 0.45 kev, and ± 0.6 kev. For air at 10 cm oil pressure, this represents a percentage error of approximately 2% for the middle of the energy range, 80 to 200 kev, and 2.5% at the high and low energy ends. Most of the gases and vapors measured in the experiment had stopping cross sections per molecule from 3/4 to $1\frac{1}{2}$ times the stopping cross section per molecule of air. This means that at the

same pressure their percentage errors are roughly the same. The principal exceptions are hydrogen and helium, which have very low stopping cross sections, and for which the percentage probable error was 4% in the middle energy region (80 to 200 kev) and 5% elsewhere. Krypton and xenon had much higher stopping cross sections, but straggling and loss of particles increased the absolute error so that the percentage error is believed to be about the same as for air.

The reading of the pressure and temperature also introduces a random error. The temperature error is small since it can be read to an accuracy of at least $\pm 0.3^{\circ}C$, and since it is the absolute temperature which is used in the calculation of the number of atoms/cm^3. This is a percentage error of 0.1%. The pressure was measured by an oil manometer with one side connected to the vacuum of the target chamber ($< 10^{-5}$ mm Hg) and the other side connected by approximately 18 inches of 1/4-inch copper and brass tube to the gas chamber. The oil level in each arm can be read with a probable error of ± 0.3mm so that the probable error of the pressure is ± 0.4 mm. 0.4 mm is an error of 1% for pressures of 4 cm oil, and 0.2% for pressures of 20 cm oil. Most gases were measured with average pressures of 10 cm so that the error is usually 0.4%. Hydrogen and helium were measured with pressures near 20 cm so that the error is 0.2%, and xenon and krypton were measured with 4 to 6 cm of oil so that the probable error is 1%.

A few measurements were taken with foils which leaked so that the pressure varied during a run which defines the gas spectrum

shown in figure 2. Points were taken in such a way that the loss of pressure made the spectrum steeper, thus minimizing its effects on the spectrum. The pressure was recorded while taking data from the center of the spectrum. This procedure was found to give measurements consistent with those taken with non-leaking foils, so that the small number of measurements taken with leaky foils are assumed to be reliable, though probably not quite as accurate as other data.

Combining these errors by the usual method, it is found that the probable error of an individual measurement due to random errors is 2.7% for xenon and krypton, 5% for hydrogen and helium and 2.5% for the other gases.

An important source of systematic error is the calibration, linearity and constancy of the energy scale of the electrostatic analyzer upon which all energy measurements are based. The analyzer is calibrated against the F^{19} $(p,\alpha\gamma)O^{16}$ resonance at $340.4 \pm .4$ kev[31] and the linearity checked by scattering the H^+, HH^+, and HHH^+ ion beams from gold into the spectrometer. The spectrometer is kept at a constant field and protons scattered at 149, 298, and 596 kev, respectively; the scattered particles should have the same energy if the analyzer is linear. Experimentally, the particles are found to have the same energy within 0.3%. The constancy of the calibration is more difficult to control and measure. The calibration is slightly affected if the analyzer is moved with respect to the electrostatic generator. It was impossible to avoid moving the analyzer slightly in lining up the target chamber and

for other reasons. The error due to moving the analyzer is believed to be very small. Probably a more important source of error is the possibility of short time variations of the beam energy due to change of temperature of the analyzer resistor stack and other similar causes. These short term effects are unmeasurable but are believed to be very small, every precaution being taken to keep them small. However, they can introduce a sizeable error in an energy loss measurement which is the difference of two energies. For this reason the probable error due to all errors in the energy scale is set at 1%.

Of the systematic errors, the next largest is the purity of the gases. Examination of Table I will show that almost all of the gases were quite pure when purchased, but contamination from various sources, particularly in connecting up the gas container to the gas chamber, is quite possible. It is difficult to determine the amount of contamination, but great care was taken to avoid any possibility of contamination. It is believed that a conservative estimate of the probable error from this cause is 0.3% for all gases except NO and N_2O, which were not as pure when purchased. The probable error for NO and N_2O is set at 0.6%.

The length of the gas cell between foil holders is measurable to 0.001 inch which is an error of only 0.04%. But the foils bulge slightly under pressure, and it is difficult to measure the amount of bulging with any accuracy. This bulging is known for each foil to $\pm$0.0025 inch, which is an error of 0.005 inch in the length of the cell or about a 0.2% probable error.

The temperature is measured by a thermometer in an oil cup fixed to the top of the target chamber. The thermometer is thus only in indirect thermal contact with the gas chamber. To determine if there is any systematic difference in temperature, another thermometer was temporarily fixed to the gas chamber; and blow torch heat was applied to the target chamber top. (see fig. 14) The temperature of both thermometers was observed over a period of half an hour, and the average difference in temperature was 0.5° C. A conservative estimate of the probable error is thus 0.2%.

The pressure measurements depend on the density of the oil. This density is very accurately measurable; but due to the possibility of dissolved gases in the oil, or other possible contamination not in the sample whose density was measured, the probable error from this source is set at 0.1%.

Taking the half-height of the spectrum as the mean energy, as has been done in this experiment, is correct only if the distribution of energy losses is Gaussian, or some other type of distribution which is symmetrical about the mean. As long as the individual energy losses of a particle are small compared to the mean energy lost, the distribution will be Gaussian. Probably the most likely sources of large energy losses to distort the loss distribution are nuclear collisions. These will contribute the largest energy losses for protons in hydrogen. Therefore, it is expected that, if there is any error introduced by taking the half-height point as the mean, it will be greatest for hydrogen. However, the total energy loss distribution is determined by the

losses in the aluminum foils as well as the gas, so that the distribution is a fold of the two distributions. The aluminum energy loss distribution is to a high degree of accuracy Gaussian. Calculation of the resulting distribution when a Gaussian is folded into a highly asymmetrical trapezoidal distribution of approximately the same width as the Gaussian, has shown that for the resulting distribution the half-height points differ from the mean by only 2%.

There is an additional possible source of asymmetrical energy loss distributions. Particles are lost from the beam by scattering, and this scattering is dependent on the energy. In general this scattering varies approximately as energy^{-2}, which means that more low energy particles will be lost than high energy. This differential loss of particles will slightly shift the measured energy spectra to higher energies with the gas spectrum being shifted slightly more than the aluminum spectrum. This will make the measured ΔE slightly greater than the actual average ΔE. If data were taken with a fixed energy entering the gas chamber and a variable energy leaving the chamber, the effect would be the opposite. The spectra would again be shifted to higher energies with the gas spectrum shifted more, but the gas spectrum would be below the foil spectrum. Because of the shift the measured ΔE would be less than the actual average ΔE. A measurement was made on argon at 65 kev, keeping the incoming energy constant and measuring the outgoing energy with the magnetic spectrometer. The energy loss measured in this latter way was 3% higher than that

previously measured. If the effects discussed in this paragraph were large enough to measure, they should have made the latter measurement lower than the previous measurements. From the results obtained, it is concluded that the differential effect of the loss of particles on the measured mean energy is negligible.

It is believed that any error introduced by an asymmetry in the spectrum shape is small unless the asymmetry is pronounced. The spectrum curves, with very few exceptions, appear to be very symmetrical so that it is believed that the probable error introduced by the assumption made regarding the mean is only 0.5%.

Due to the unfortunate appearance of non-reproducible results for a few gases at low energy, an additional probable error must be added to the cross section in the energy range below 125 kev. This additional probable error is arbitrarily set at 2%. (See Section IV, p. 34)

The random errors discussed in the first part of this section apply to one individual measurement. It is now necessary to assess the influence of the error in the individual measurements on the error in the finally adopted cross section values. If the analytical form of the cross section function were known, the cross section would be determined by the method of least squares; and the error at any one point would be proportional to the square root of the number of measurements taken. The analytical form is not known, however, so that the procedure used involved drawing by eye a smooth curve to fit the experimental points. The curve at any one point is then influenced primarily by those measurements nearest the point in question and to a lesser extent by measurements

further away. It is estimated that the effective number of measurements which determine the value of the curve at any one energy is four. In this way, the probable error of the finally adopted value of the stopping cross section is believed to be one-half the average random error of an individual measurement.

The probable error from all causes discussed above is calculated for all gases and presented in Table VI. The error in carbon is determined by combining the errors of the hydrocarbons and CO_2 with that for hydrogen and dividing by the square root of five to account for the five determinations. The resulting error is that found assuming Bragg's rule to be valid.

VI STRAGGLING

Bohr's simple classical theory[32] gives for the energy straggling of protons:

$$\Omega^2 = N\,dx\,K\,T_m\,Z$$

where $K = \frac{2\pi e^4}{m v^2}$, $T_m = 2 m v^2$, and therefore

$$\Omega^2 = N\,dx\,k\,Z$$

where k is a constant = $4\pi e^4$

More accurate calculations of Livingston and Bethe[18], which take account of the high binding energies of the inner electrons, show that Z should be replaced by:

$$Z_{eff} = Z' + \sum_n \gamma_n \frac{I_n Z_n}{m v^2} \ln \frac{2 m v^2}{I_n}$$

where Z' is the number of electrons in the atom which are "effective" in the stopping, that is, whose binding energy is less than $\frac{mE}{M}$ and is defined more exactly by Bethe[18]. Z_n is the number of electrons in the n^{th} shell; I_n is the average excitation energy in the n^{th} shell; and γ_n is a constant, different for each shell but all $\gamma_n \approx 4/3$.

For the energies of this experiment, Z_{eff} is definitely different from Z; but it is not a rapidly varying function of energy, since Z' decreases with energy and the summation term increases with a decrease in energy. Since Z_{eff} is equal to Z for high energies, we can see that Z_{eff} will stay of the same order of magnitude as Z.

Figure 13 shows the straggling found for krypton and xenon plotted as ω^2 versus energy where $\omega^2 = \Omega^2/Ndx$ The dotted line shows for comparison the value predicted by Bohr's simple theory.

From figure 13, it can be seen:

1. This experiment is not a good way to measure the straggling.

2. The straggling found is of the same order of magnitude as that predicted theoretically.

TABLE I

GAS SUPPLIERS AND PURITY

Gas	Manufacturer	Purity	Principle Impurity
H	Linde Air Products	99.5%	
He	Air Reduction Co.	99.7%	
Ne	Air Reduction Sales Co.	99.996%	
Ar	Linde Air Products	99.92%	N_2
Kr	Air Reduction Sales Co.	99.996%	
Xe	Air Reduction Sales Co.	99.996%	
N_2	Linde Air Products	99.92%	
O_2	Linde Air Products	99.5%	
NO	Mathieson Chemical Co.	98.7%	Higher oxides of N and N_2
N_2O	Ohio Chemical Co.	98%	N_2
NH_3	Dow Chemical Co.	99.95%	
CO_2	Ohio Chemical Co.	99.7%	
H_2O	Distilled Water	99.9%	
C_6H_6	Baker and Adamson	99.98%	H_2O
CH_4	Texas Co.	Impurity .002 mole fractions (not including H_2O)	H_2O
C_2H_4	Ohio Chemical Co.	99.5%	
C_2H_2	Linde Air Products	99.62%	Acetone

TABLE II

PROTON STOPPING CROSS SECTION PER ATOM (10^{-15} ev-cm^2)

Energy (kev)	$\frac{1}{2}H_2$	He	$\frac{1}{2}N_2$	$\frac{1}{2}O_2$	$\frac{1}{2}Air_2$	C	A	Ne	Kr	Xe
30	5.84		16.1		15.50					
40	6.25	6.67	17.1	15.2	16.48		31.4	10.6	35.6	50.0
50	6.43	6.97	17.8	16.4	17.16		33.4	11.9	38.3	52.6
60	6.45	7.22	18.2	16.9	17.70		34.3	12.8	39.8	53.5
70	6.36	7.33	18.5	17.15	17.90		34.4	13.45	40.5	53.5
80	6.23	7.37	18.5	17.25	17.87		34.1	13.95	40.5	53.2
90	6.04	7.37	18.25	17.25	17.72		33.5	14.3	40.3	52.0
100	5.83	7.30	17.9	17.17	17.50	16.25	32.6	14.6	39.8	50.6
150	4.70	6.37	16.1	16.13	15.98	14.6	28.2	14.6	35.0	45.2
200	3.90	5.55	14.2	14.70	14.21	12.70	24.5	14.10	30.7	41.8
250	3.33	4.91	12.5	13.26	12.71	11.28	21.6	13.20	27.4	38.6
300	2.91	4.41	11.2	11.99	11.56	10.20	19.5	12.34	25.1	35.8
350	2.60	4.01	10.13	11.01	10.60	9.30	17.9	11.50	23.3	33.4
400	2.35	3.69	9.34	10.23	9.79	8.54	16.6	10.75	22.0	31.4
450	2.14	3.42	8.62	9.45	9.05	7.94	15.55	10.15	20.9	29.8
500	1.97	3.18	8.08	8.84	8.39	7.38	14.7	9.58	19.9	28.6
550	1.82	2.99	7.61	8.38	7.90	6.95	13.9	9.09	19.1	27.4
600	1.70	2.81	7.21	7.91	7.51	6.55	13.3	8.65	18.4	26.4

TABLE III

PROTON STOPPING CROSS SECTION PER MOLECULE (10^{-15} ev-cm^2)

Energy (kev)	CH_4	C_2H_2	C_2H_4	C_6H_6	H_2O	NH_3	NO	CO_2	N_2O
30	37.4	43.4		116.0		29.7			
40	39.7	47.4	54.4	126.0	25.0	32.0	32.6	44.2	47.0
50	40.9	49.5	57.4	133.0	26.1	33.6	34.5	46.8	48.6
60	41.3	49.8	58.7	135.7	26.9	34.6	35.7	48.4	49.9
70	41.2	49.2	58.8	135.5	27.5	34.7	36.4	49.6	50.5
80	40.8	48.0	58.0	134.4	27.6	34.4	36.6	50.2	50.9
90	40.0	46.7	56.7	133.5	27.5	33.9	36.6	50.5	51.0
100	38.9	45.0	55.5	131.7	27.3	33.5	36.4	50.5	50.7
150	33.6	38.5	48.8	116.5	24.7	30.1	33.2	47.1	47.0
200	28.6	32.9	41.4	102.0	22.0	25.6	29.7	42.5	42.0
250	24.8	29.0	36.1	89.2	19.7	22.3	26.7	38.1	37.6
300	22.0	25.9	32.0	79.8	17.9	19.9	24.1	34.6	34.0
350	19.8	23.5	28.8	72.2	16.2	17.9	22.0	31.6	31.0
400	18.1	21.4	26.2	66.3	15.0	16.4	20.3	29.2	28.6
450	16.65	19.7	24.1	61.4	13.9	15.1	18.9	27.0	26.6
500	15.5	18.4	22.4	57.3	13.0	14.0	17.6	25.2	25.0
550	14.5	17.2	20.9	53.9	12.2	13.1	16.6	23.7	23.5
600	13.6	16.2	19.6	51.0		12.3	15.7	22.4	22.2

TABLE IV

DIFFERENTIAL ATOMIC STOPPING POWER

E (kev)	$\frac{1}{2}H_2$	He	$\frac{1}{2}N_2$	$\frac{1}{2}O_2$	C	A	Ne	Kr	Xe
30	.377		1.04						
40	.379	.404	1.04	.922		1.905	.644	2.16	3.03
50	.375	.406	1.04	.966		1.948	.694	2.23	3.065
60	.364	.407	1.03	.955		1.940	.724	2.25	3.02
70	.355	.409	1.035	.959		1.920	.752	2.265	2.99
80	.348	.411	1.035	.965		1.908	.781	2.27	2.98
90	.341	.416	1.03	.974		1.890	.807	2.275	2.935
100	.333	.417	1.024	.982	.929	1.863	.835	2.275	2.89
150	.294	.398	1.01	1.01	.914	1.764	.914	2.19	2.83
200	.275	.390	1.00	1.035	.894	1.723	.993	2.16	2.94
250	.261	.385	.982	1.04	.885	1.695	1.035	2.15	3.03
300	.252	.381	.970	1.035	.883	1.690	1.07	2.17	3.10
350	.245	.378	.955	1.04	.878	1.690	1.085	2.20	3.15
400	.240	.377	.955	1.045	.873	1.696	1.10	2.25	3.21
450	.237	.378	.953	1.045	.878	1.720	1.12	2.31	3.29
500	.235	.379	.964	1.053	.880	1.750	1.14	2.37	3.41
550	.231	.379	.964	1.063	.881	1.760	1.15	2.42	3.47
600	.227	.374	.961	1.055	.873	1.775	1.15	2.45	3.52

TABLE V

DIFFERENTIAL MOLECULAR STOPPING POWER

Energy (kev)	CH_4	C_2H_2	C_2H_4	C_6H_6	H_2O	NH_3	NO	CO_2	N_2O
30	2.41	2.80		7.49		1.92			
40	2.41	2.88	3.30	7.55	1.52	1.94	1.98	2.68	2.85
50	2.38	2.89	3.35	7.75	1.52	1.96	2.01	2.73	2.83
60	2.33	2.82	3.32	7.67	1.52	1.955	2.02	2.73	2.82
70	2.30	2.75	3.28	7.57	1.54	1.94	2.03	2.77	2.82
80	2.28	2.69	3.24	7.52	1.54	1.92	2.05	2.81	2.84
90	2.26	2.63	3.20	7.54	1.55	1.91	2.06	2.85	2.88
100	2.22	2.57	3.17	7.53	1.56	1.91	2.08	2.88	2.89
150	2.10	2.41	3.05	7.29	1.545	1.88	2.08	2.95	2.94
200	2.01	2.32	2.91	7.18	1.55	1.80	2.09	2.99	2.96
250	1.95	2.27	2.83	7.00	1.55	1.75	2.02	2.99	2.95
300	1.90	2.24	2.77	6.91	1.55	1.72	2.08	2.99	2.94
350	1.87	2.22	2.72	6.82	1.53	1.69	2.08	2.98	2.92
400	1.85	2.18	2.68	6.78	1.53	1.675	2.07	2.98	2.92
450	1.84	2.18	2.66	6.79	1.54	1.67	2.09	2.98	2.94
500	1.85	2.19	2.67	6.84	1.55	1.67	2.10	3.00	2.98
550	1.84	2.18	2.65	6.83	1.545	1.66	2.10	3.00	2.97
600	1.81	2.16	2.61	6.81		1.64	2.09	2.99	2.96

TABLE VI

PROBABLE ERRORS

Gases	30 - 100 kev	100 - 600 kev
Air, nitrogen, oxygen, H_2O, C_2H_2, C_2H_4 CH_4, C_6H_6, CO_2, NH_3, Argon, neon	2.6%	1.7%
NO and N_2O	2.8%	1.9%
Krypton and xenon	2.7%	1.8%
Hydrogen and helium	3.4%	2.7%
Carbon	-	2.1%

DESCRIPTION OF FIGURES

Figure 1 Schematic diagram of the gas cell used in the experiment.

Figure 2 Illustration of experimental data from which energy loss is determined.

Figure 3 The stopping cross section for oxygen nitrogen, helium, and hydrogen.

Figure 4 The proton stopping cross section for N_2O, NO, and H_2O, compared with that calculated by Bragg's rule from the stopping cross sections of N_2, O_2, and H_2. The stopping cross section for D_2O ice as measured by Wenzel and Whaling.

Figure 5 The stopping cross section for protons of CO_2 and NH_3, and that calculated by Bragg's rule for NH_3.

Figure 6 The proton stopping cross section for four hydrocarbons, and illustrating the usual number of experimental points taken.

Figure 7 The stopping cross section for protons of carbon as derived from five carbon-containing compounds, by using Bragg's rule to subtract the stopping cross section of the atoms in the compound.

Figure 8 The proton stopping cross section of carbon and hydrogen. The solid line for carbon is the average of the curves shown in figure 7. The solid line for hydrogen is that determined directly by experiment. The dashed curves are found by taking five pairs of hydrocarbons and determining both hydrogen and carbon by subtraction and then averaging the results.

Figure 9 The stopping cross section for protons in air illustrating the scatter of a great many points.

Figure 10 The proton range in air, calculated from the stopping cross section data of this experiment. The dashed line is the range-energy curve given by Bethe[11], which was arranged to agree with the cloud chamber range measurements shown for the reactions $N^{14}(n,p)C^{14}$ and $He^{3}(n,p)T^{3}$ measured with thermal neutrons. The range is adjusted to fit that of Bethe at 20 kev.

Figure 11 Proton stopping cross section of krypton, xenon, neon and argon.

Figure 12 Comparison of results for the stopping cross section of argon from four different laboratories.

Figure 13 Experimental data of this experiment on the straggling cross section of xenon and krypton.

Figure 14 Diagram of the target chamber and gas chamber.

Figure 15 through 31 Individual graphs of the experimental points and smooth curves for each of the gases measured.

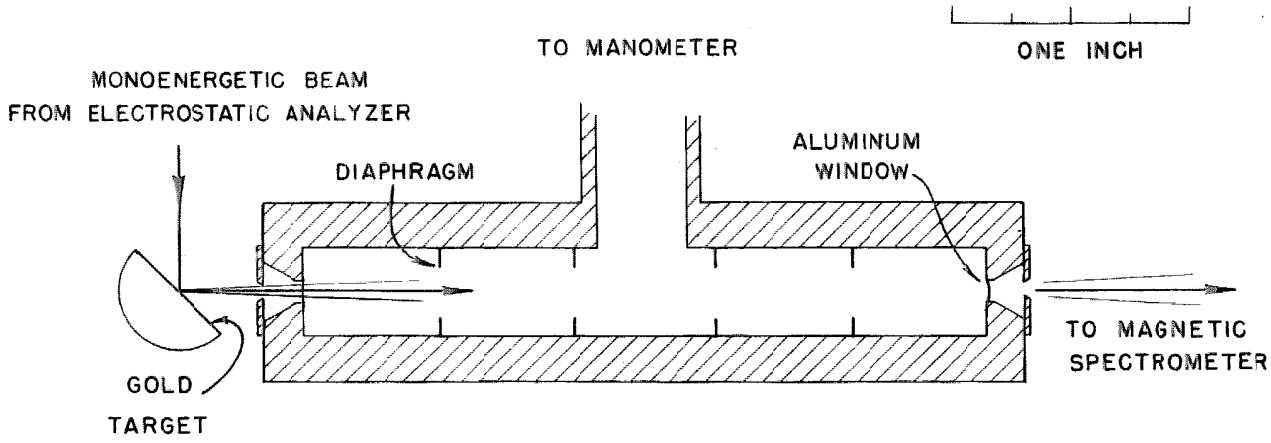

GAS CELL

fig. 1

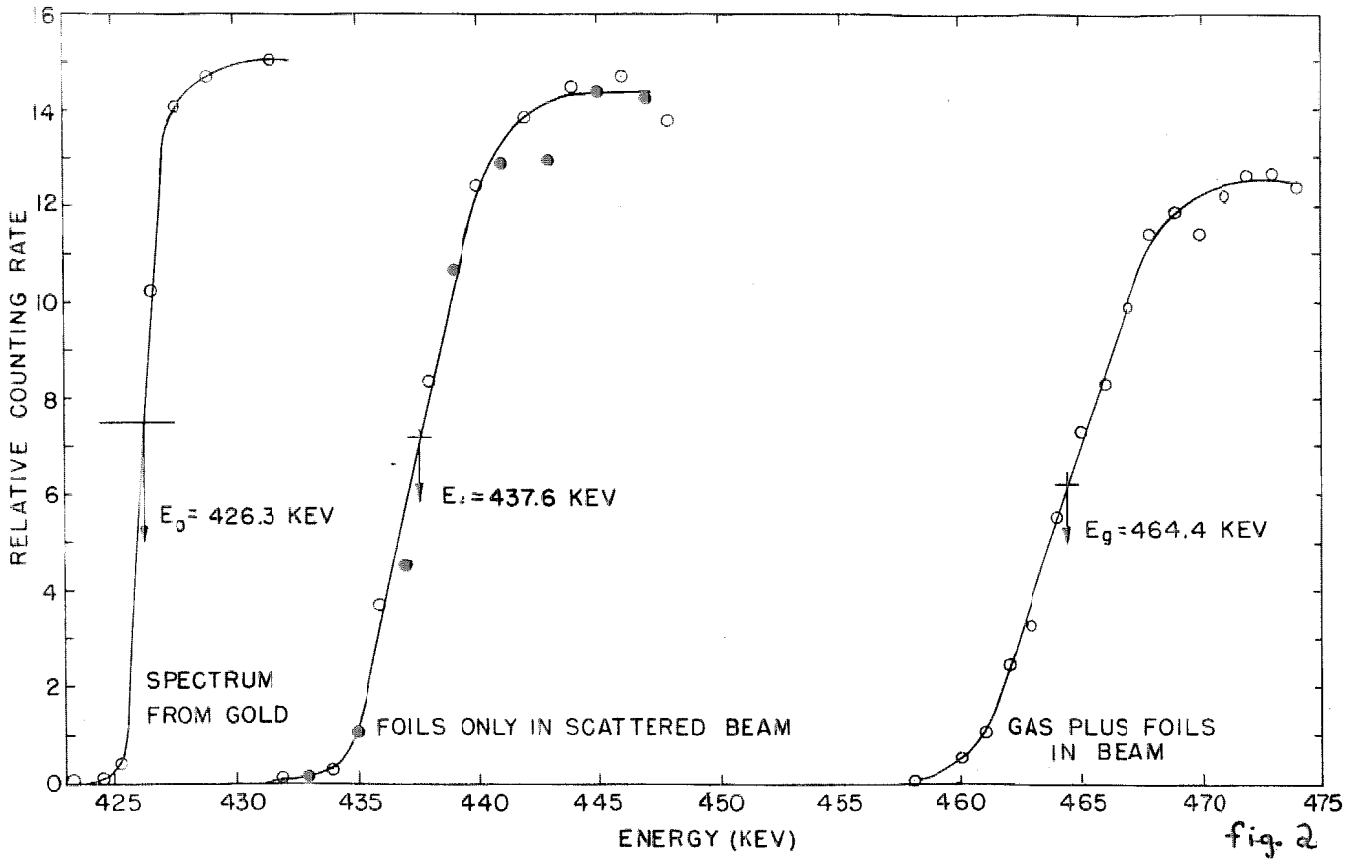
RELATIVE COUNTING RATE
ENERGY (KEV)
E_0 = 426.3 KEV
E_1 = 437.6 KEV
E_g = 464.4 KEV
SPECTRUM FROM GOLD
FOILS ONLY IN SCATTERED BEAM
GAS PLUS FOILS IN BEAM

fig. 2

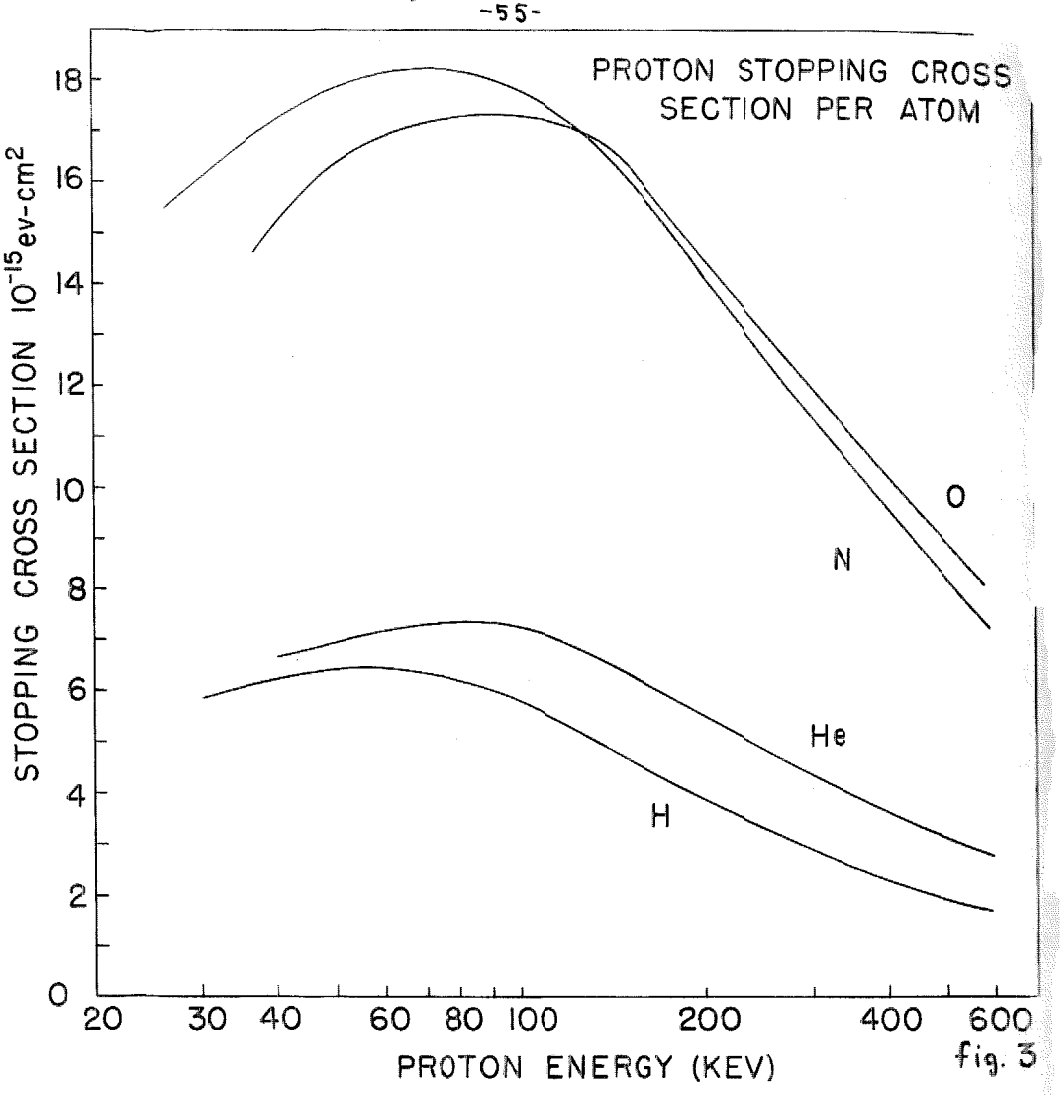
PROTON STOPPING CROSS SECTION PER ATOM
STOPPING CROSS SECTION 10^{-15} ev-cm^2
0
2
4
6
8
10
12
14
16
18
20
30
40
60
80
100
200
400
600
PROTON ENERGY (KEV)
O
N
He
H

fig. 3

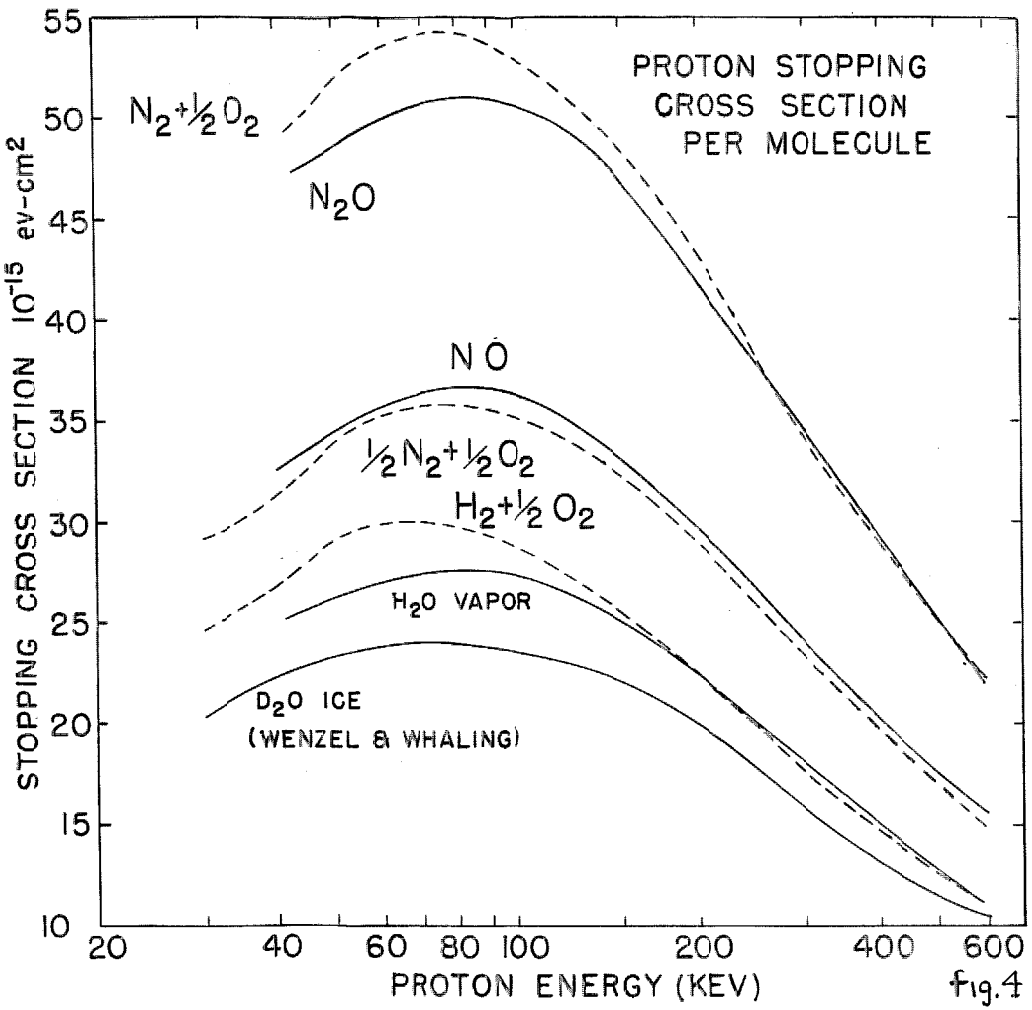
PROTON STOPPING
CROSS SECTION
PER MOLECULE
$N_2+\frac{1}{2}O_2$
N_2O
NO
$\frac{1}{2}N_2+\frac{1}{2}O_2$
$H_2+\frac{1}{2}O_2$
H_2O VAPOR
D_2O ICE
(WENZEL & WHALING)
STOPPING CROSS SECTION 10^{-15} ev-cm^2
PROTON ENERGY (KEV)
55
50
45
40
35
30
25
20
15
10
20
40
60
80
100
200
400
600

fig.4

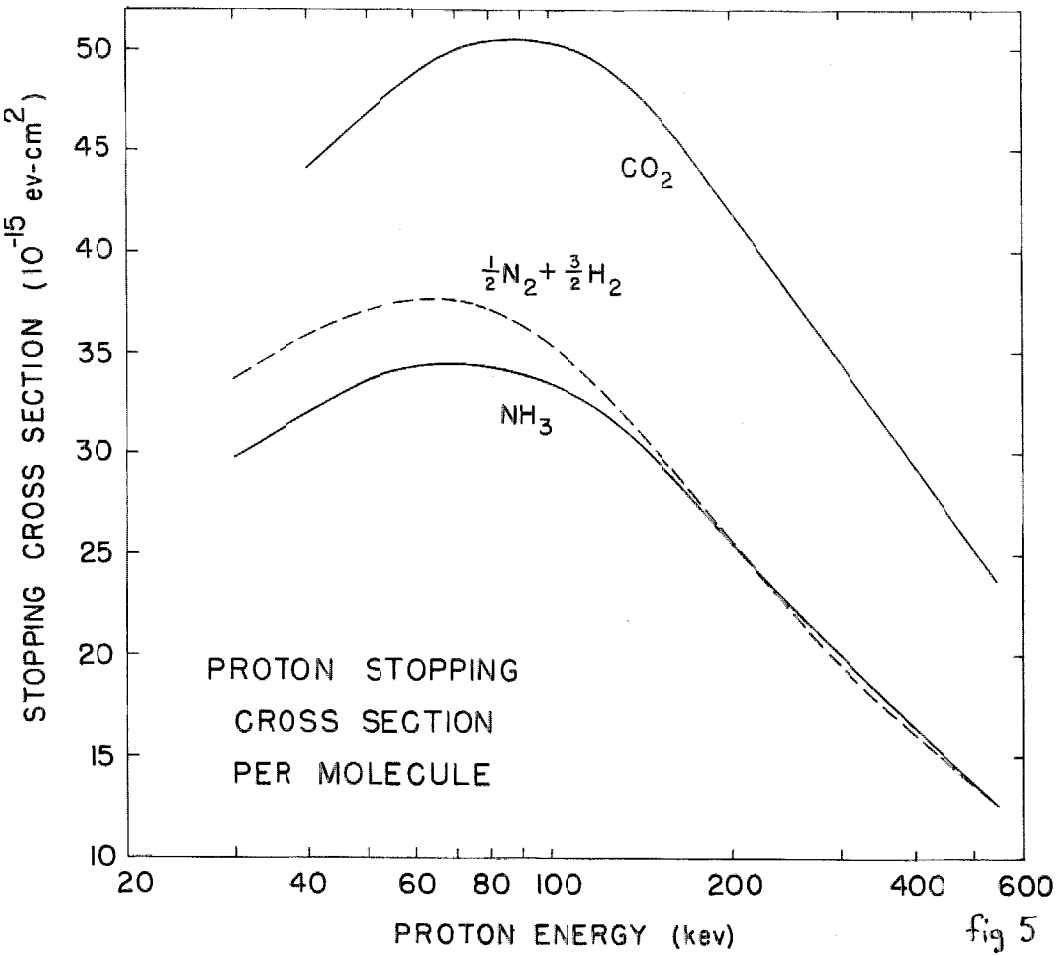
STOPPING CROSS SECTION (10^{-15} ev-cm^2)
50
45
40
35
30
25
20
15
10
CO_2
$\frac{1}{2}N_2+\frac{3}{2}H_2$
NH_3
PROTON STOPPING
CROSS SECTION
PER MOLECULE
20
40
60
80
100
200
400
600
PROTON ENERGY (kev)

fig 5

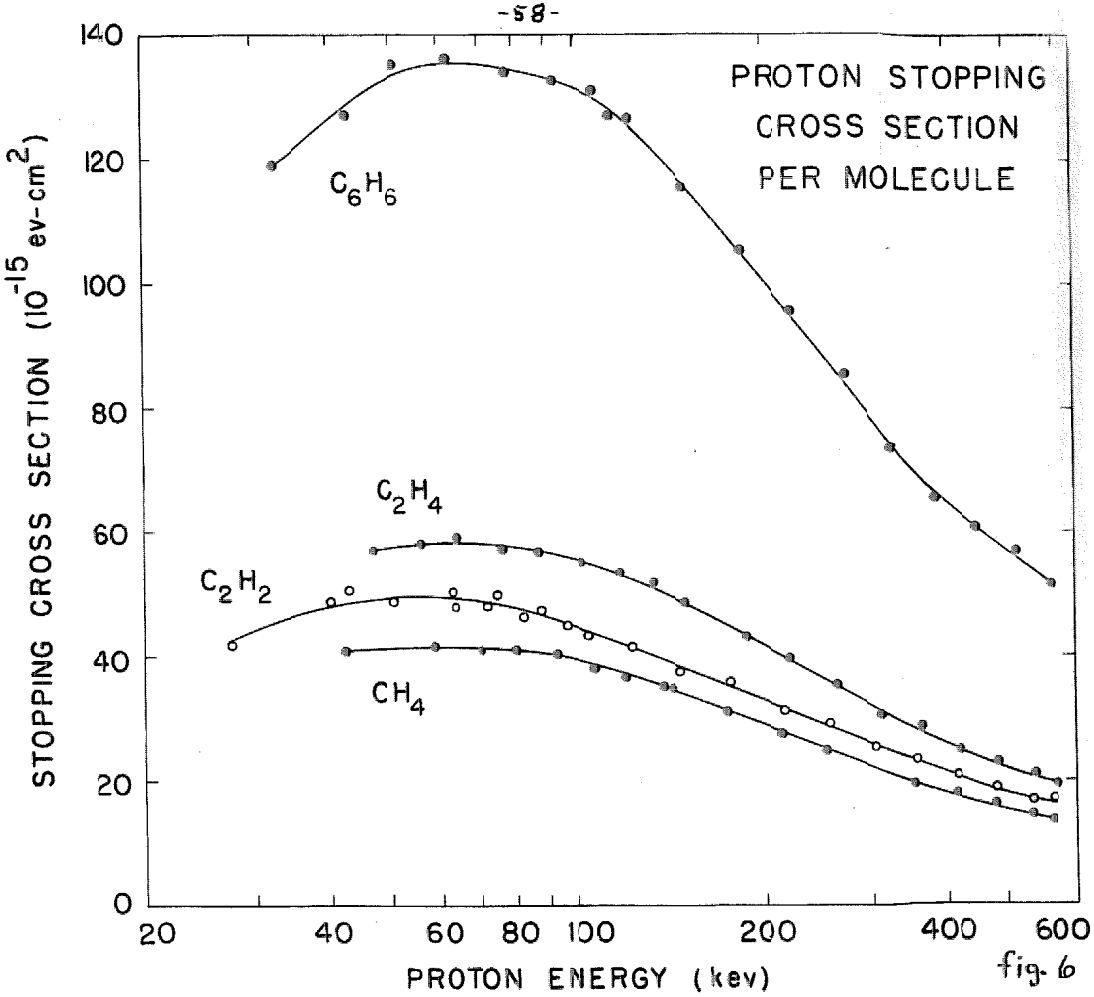
PROTON STOPPING
CROSS SECTION
PER MOLECULE
C_6H_6
C_2H_4
C_2H_2
CH_4
STOPPING CROSS SECTION (10^{-15} ev-cm^2)
PROTON ENERGY (kev)
0
20
40
60
80
120
140
100
200
400
600

fig. 6

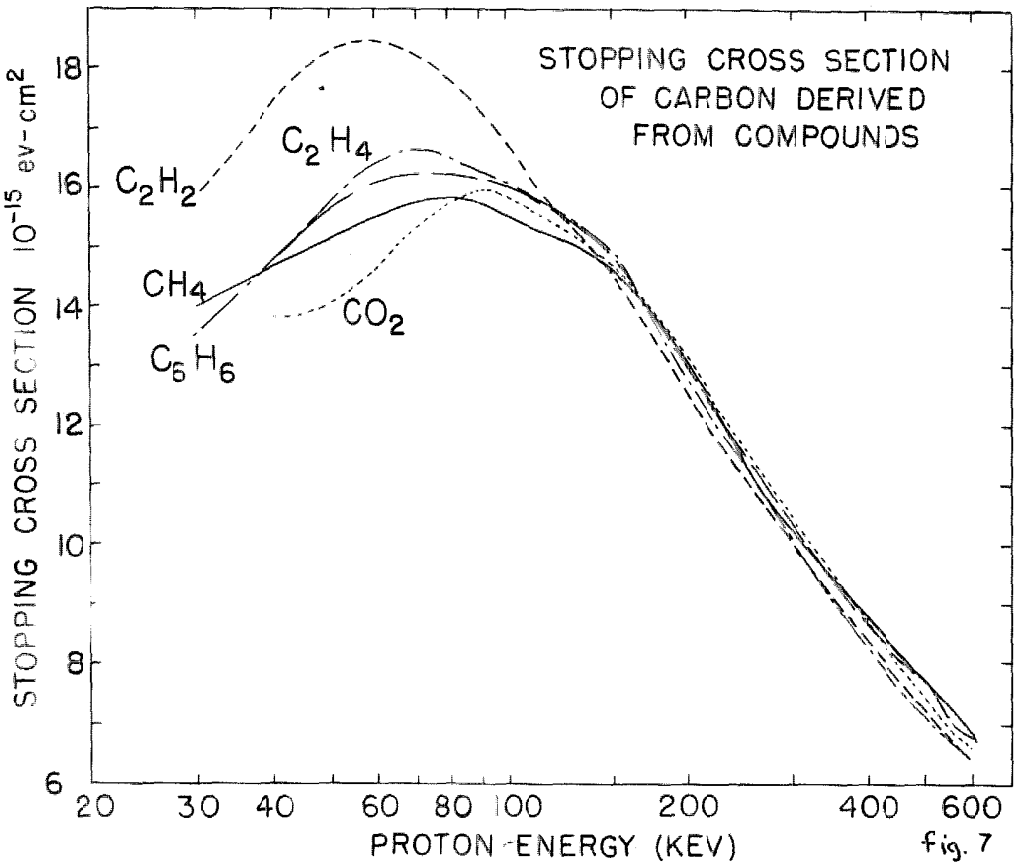
STOPPING CROSS SECTION OF CARBON DERIVED FROM COMPOUNDS
C_2H_2
C_2H_4
CH_4
CO_2
C_6H_6
STOPPING CROSS SECTION 10^{-15} ev-cm^2
18
16
14
12
10
8
6
20
30
40
60
80
100
200
400
600
PROTON ENERGY (KEV)

fig. 7

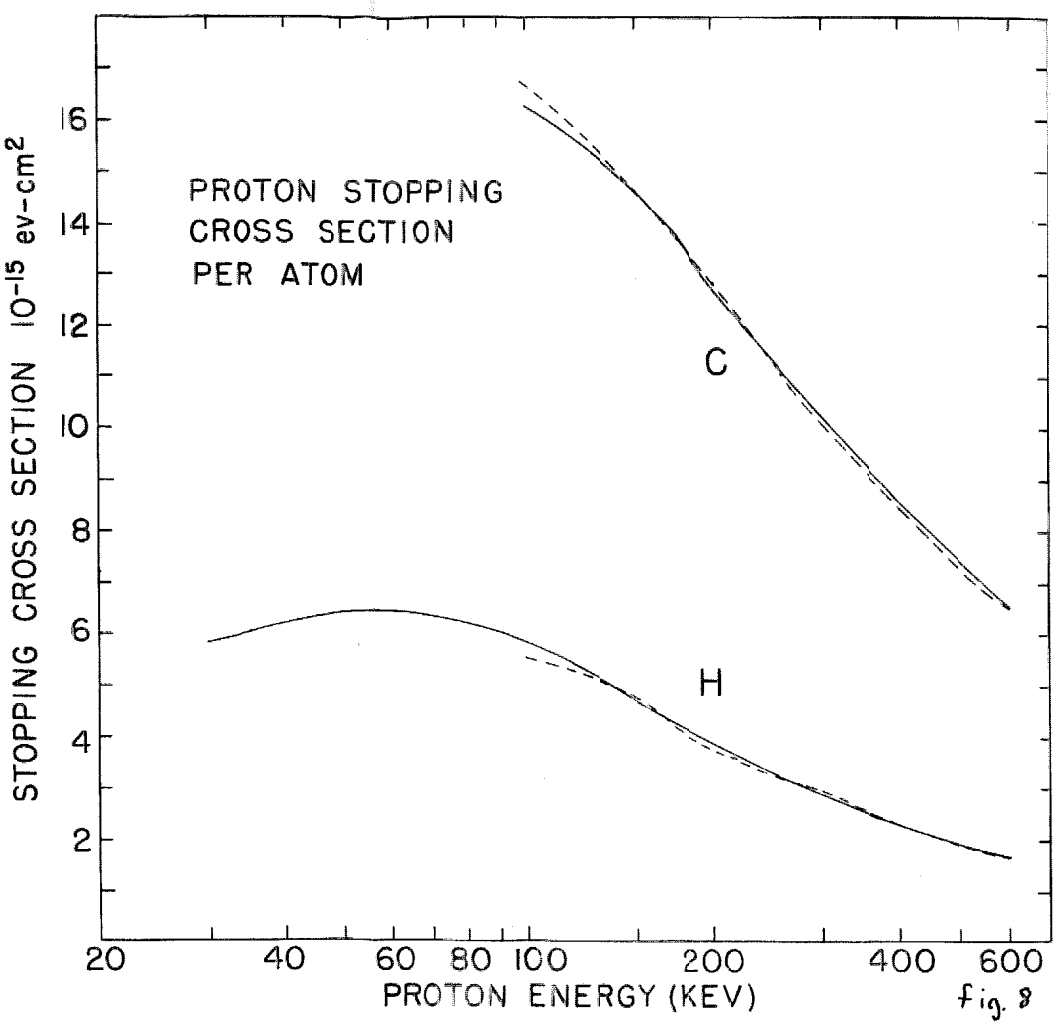
PROTON STOPPING
CROSS SECTION
PER ATOM
C
H
STOPPING CROSS SECTION 10-15 ev-cm2
16
14
12
10
8
6
4
2
20
40
60
80
100
200
400
600
PROTON ENERGY (KEV)

fig. 8

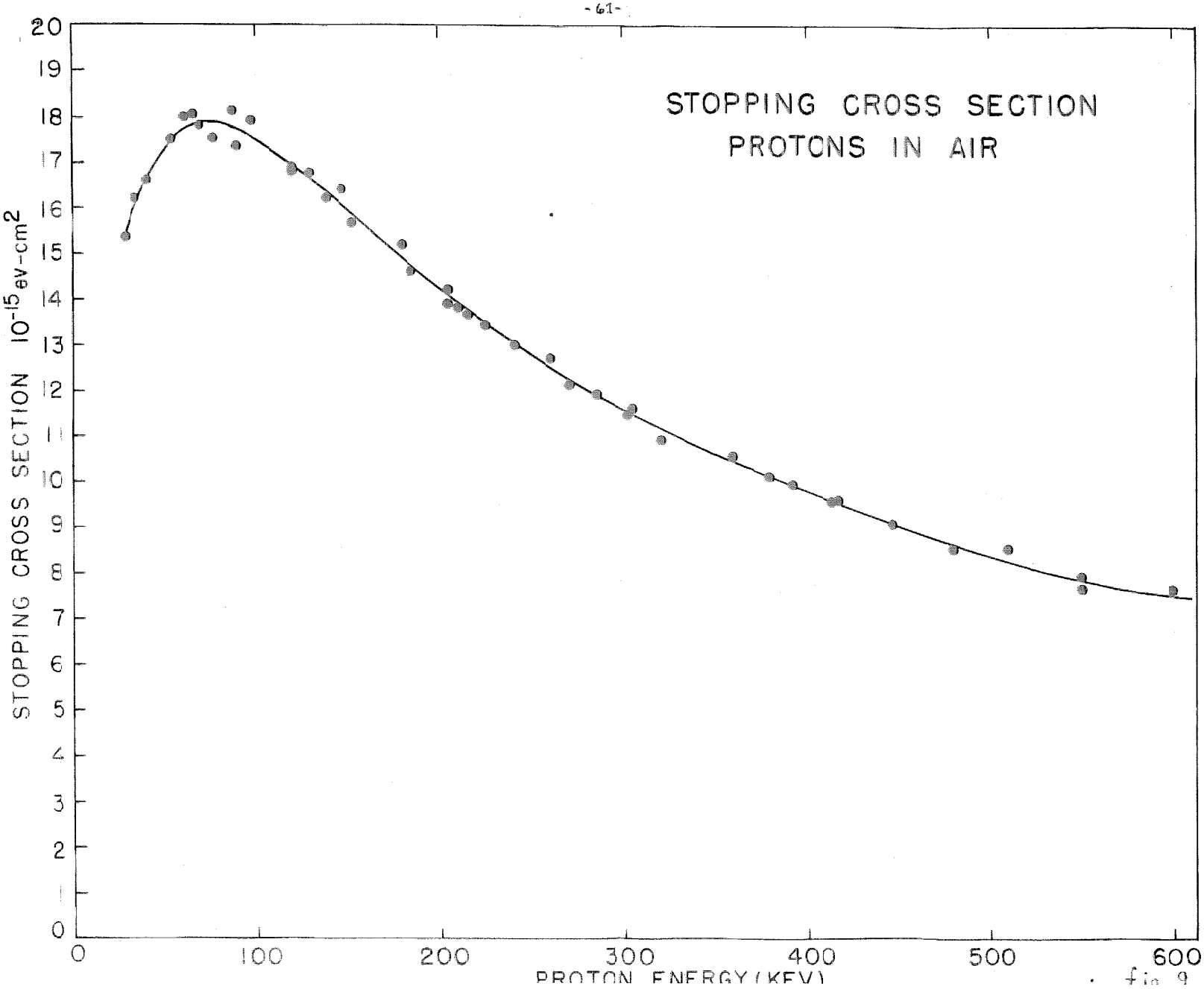
STOPPING CROSS SECTION
PROTONS IN AIR
STOPPING CROSS SECTION 10^{-15} ev-cm^2
0
2
3
4
5
6
7
8
9
10
11
12
13
14
15
16
17
18
19
20
0
100
200
300
400
500
600
PROTON ENERGY (KEV)

fig 9

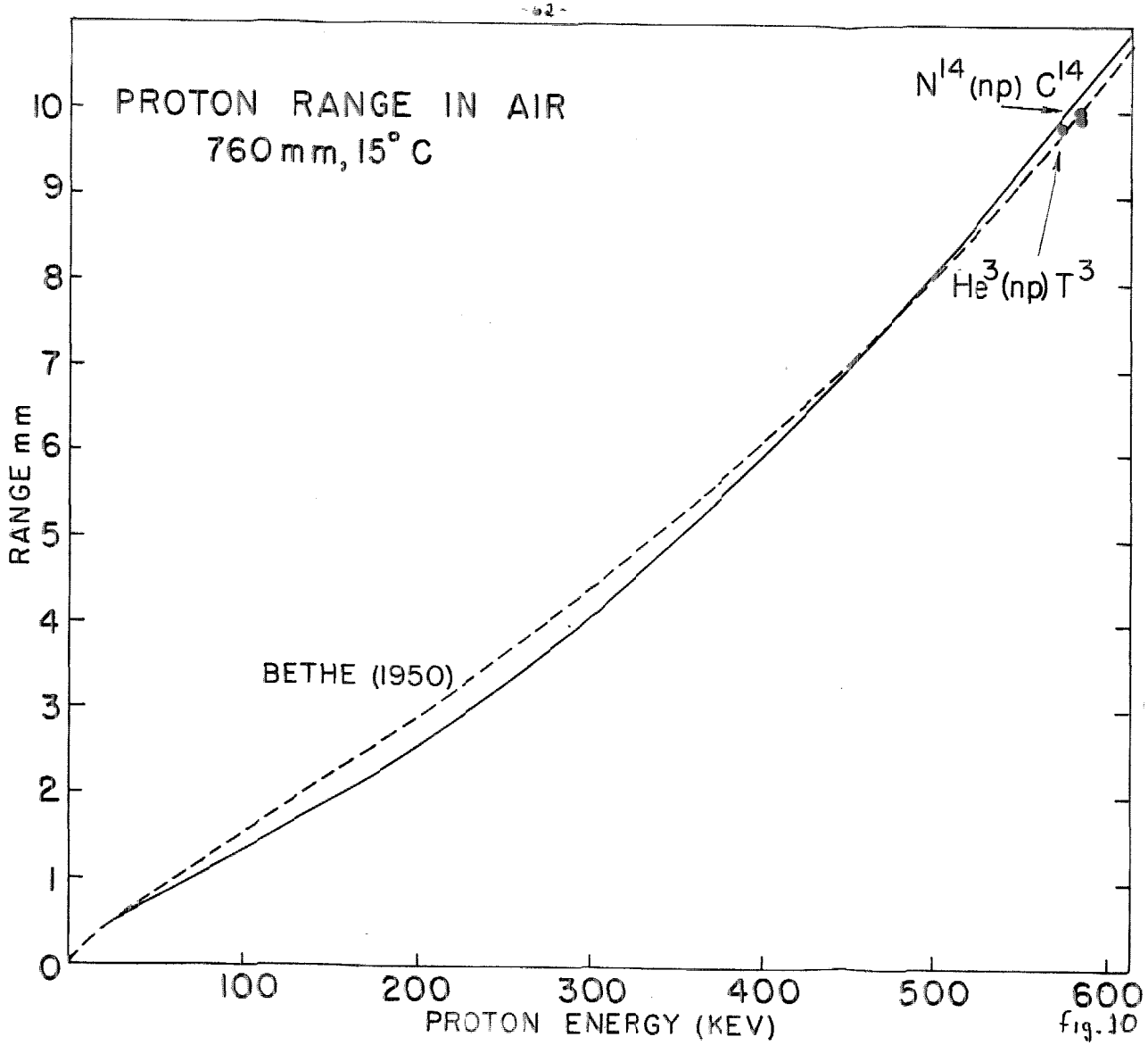
PROTON RANGE IN AIR
760 mm, 15° C
N^{14}(np) C^{14}
He^3(np) T^3
BETHE (1950)
RANGE mm
PROTON ENERGY (KEV)
0
1
2
3
4
5
6
7
8
9
10
100
200
300
400
500
600

fig. 10

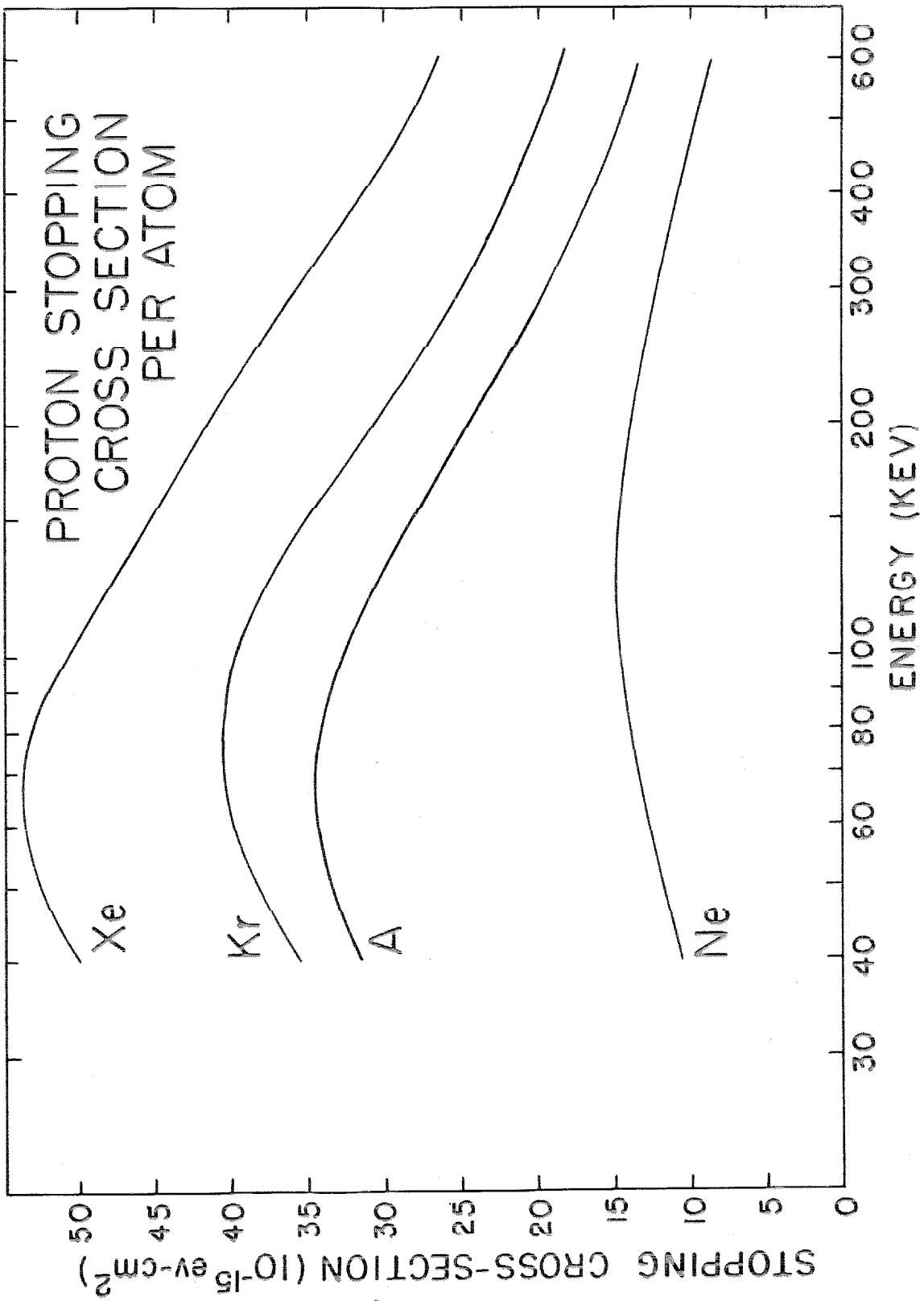
PROTON STOPPING
CROSS SECTION
PER ATOM
Xe
Kr
A
Ne
STOPPING CROSS-SECTION (10^{-15} ev-cm^2)
ENERGY (KEV)
0
5
10
15
20
25
30
35
40
45
50
30
40
60
80
100
200
300
400
600

fig. 11

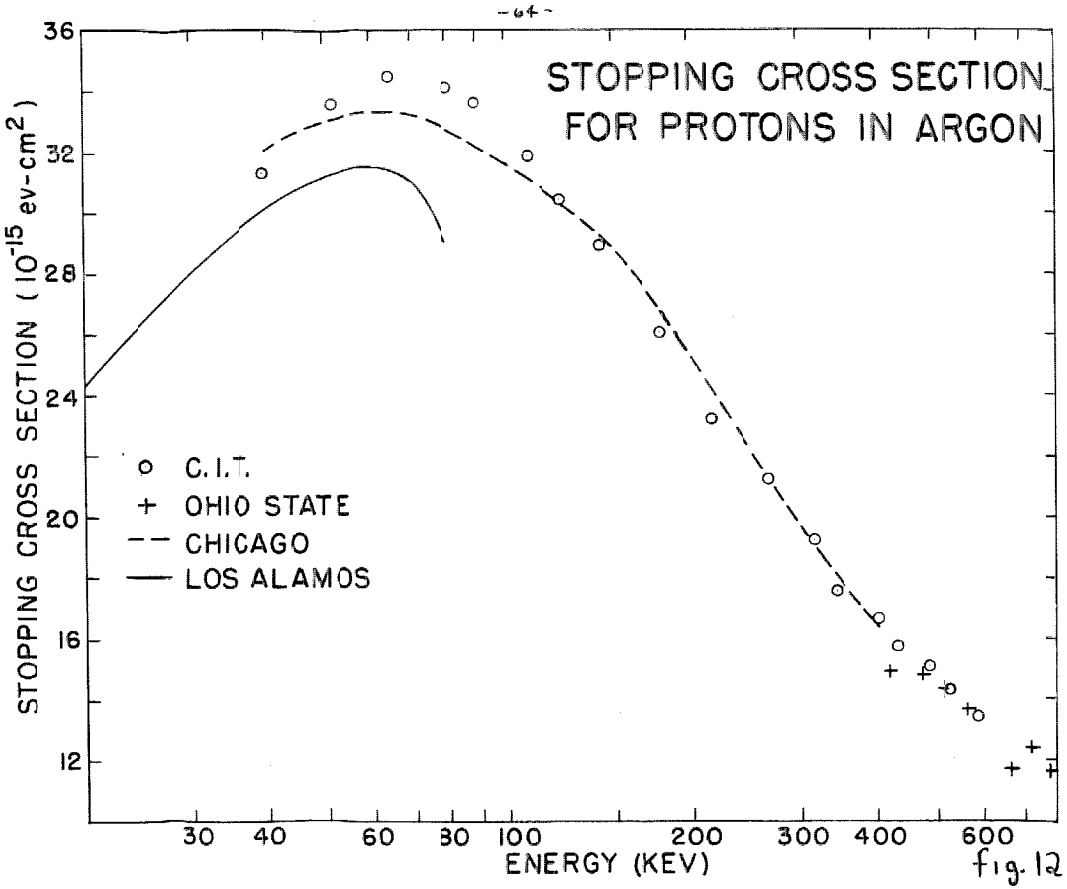
STOPPING CROSS SECTION
FOR PROTONS IN ARGON
STOPPING CROSS SECTION (10^{-15} ev-cm^2)
36
32
28
24
20
16
12
C.I.T.
OHIO STATE
CHICAGO
LOS ALAMOS
30
40
60
80
100
200
300
400
600
ENERGY (KEV)

fig. 12

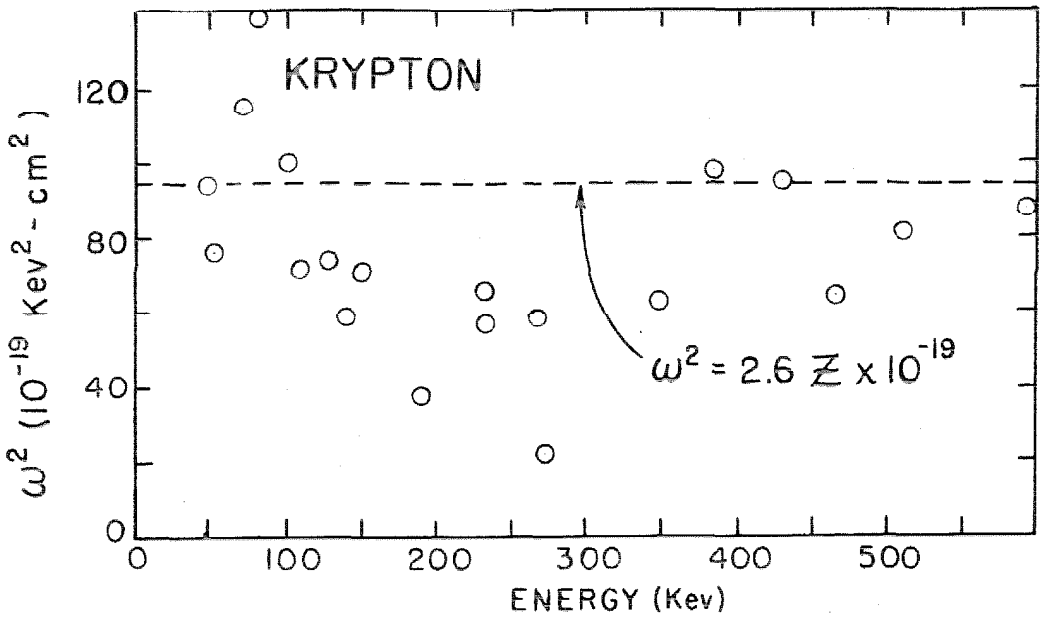

STRAGGLING CROSS-SECTION

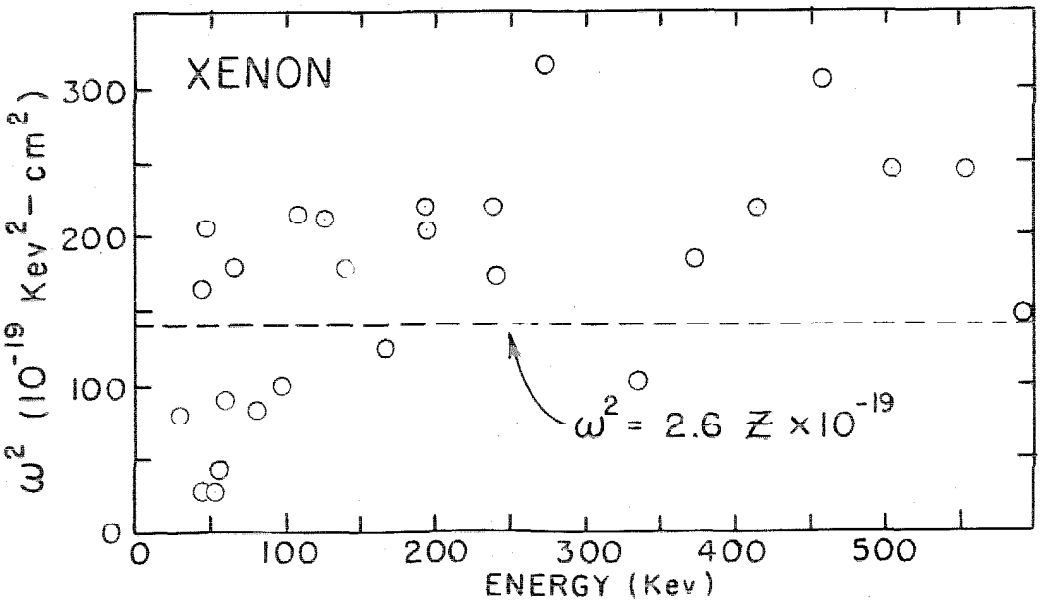

fig. 13

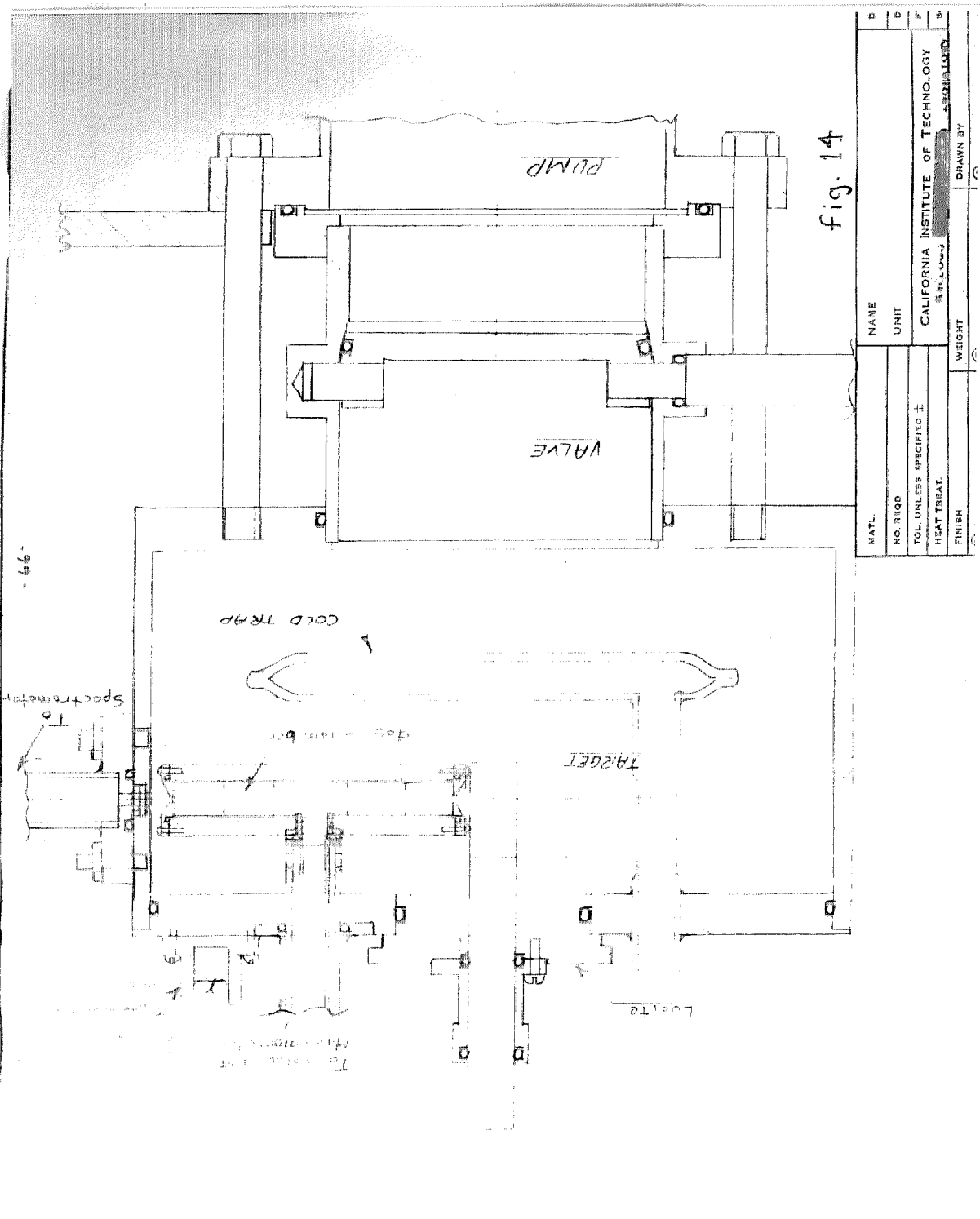
PUMP
VALVE
COLD TRAP
TARGET
To Spectrometer
CALIFORNIA INSTITUTE OF TECHNOLOGY
NAME
UNIT
MATL.
NO. REQD
TOL. UNLESS SPECIFIED ±
HEAT TREAT.
FINISH
WEIGHT
DRAWN BY

fig. 14

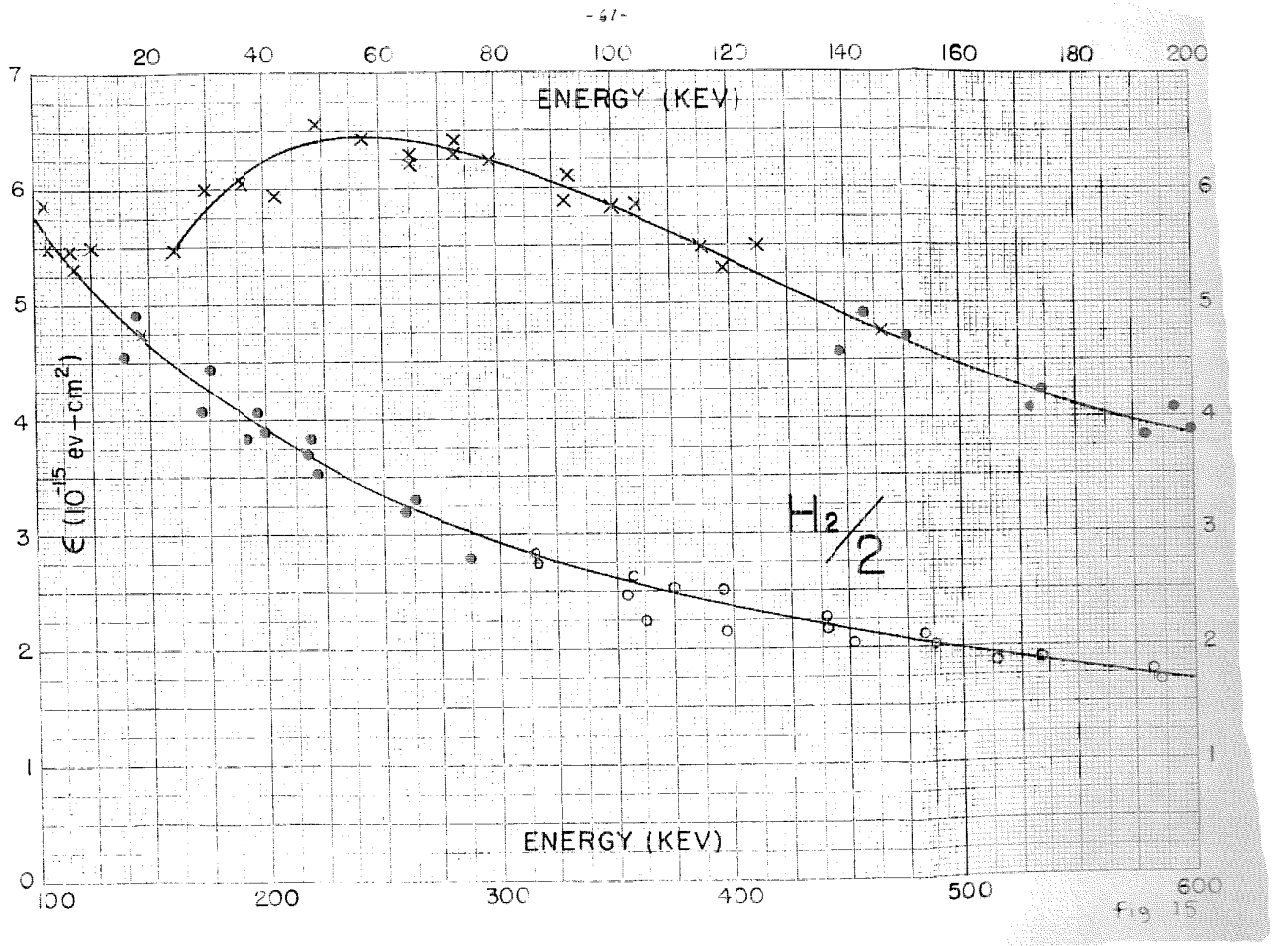
20
40
60
80
100
120
140
160
180
200
ENERGY (KEV)
ϵ (10^{-15} ev-cm^2)
$H_2/2$
ENERGY (KEV)
100
200
300
400
500
600
0
1
2
3
4
5
6
7

Fig 15

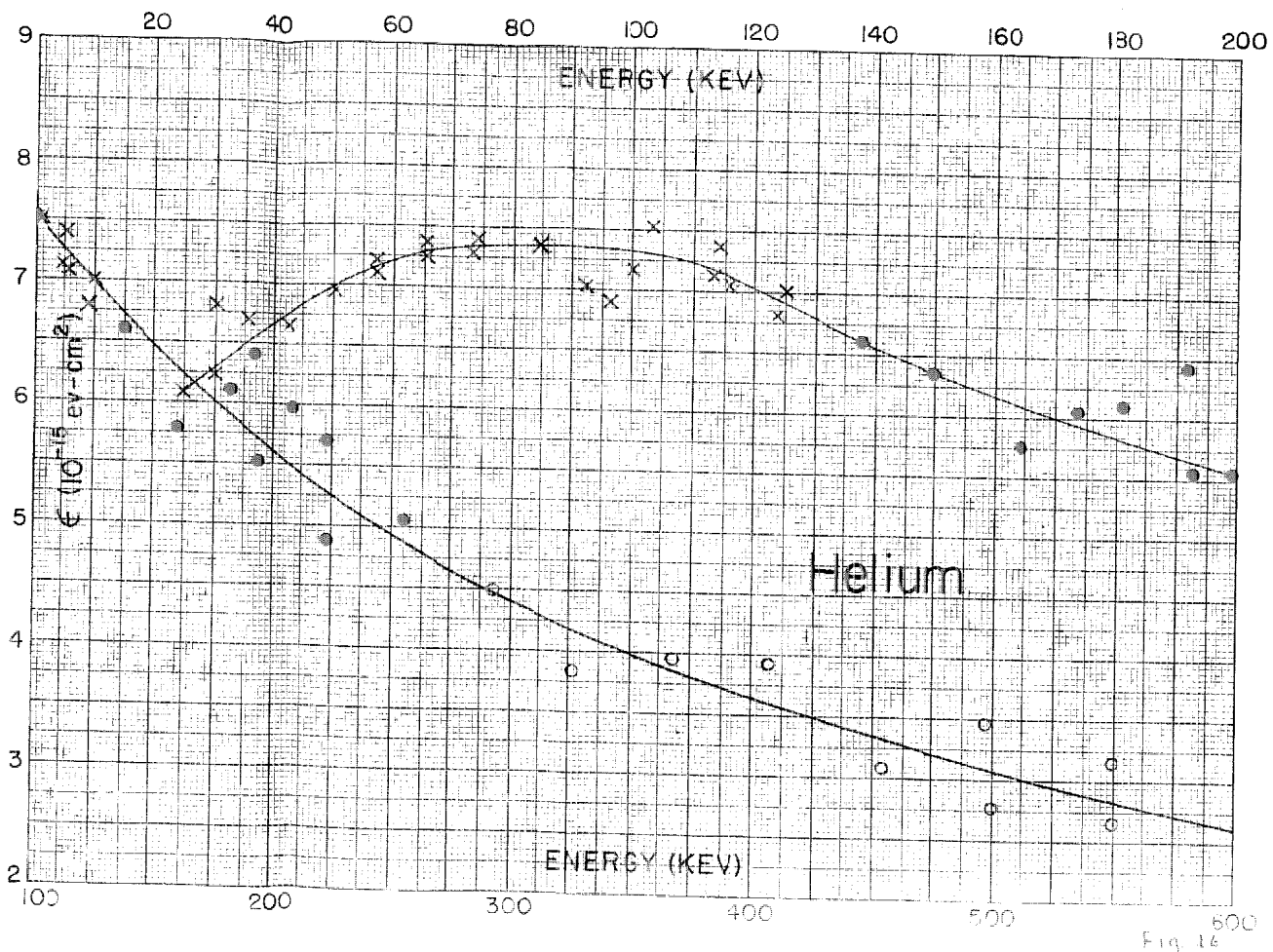
20
40
60
80
100
120
140
160
180
200
ENERGY (KEV)
9
8
7
6
5
4
3
2
ε (10⁻¹⁵ ev-cm²)
Helium
100
200
300
400
500
600
ENERGY (KEV)

Fig. 16

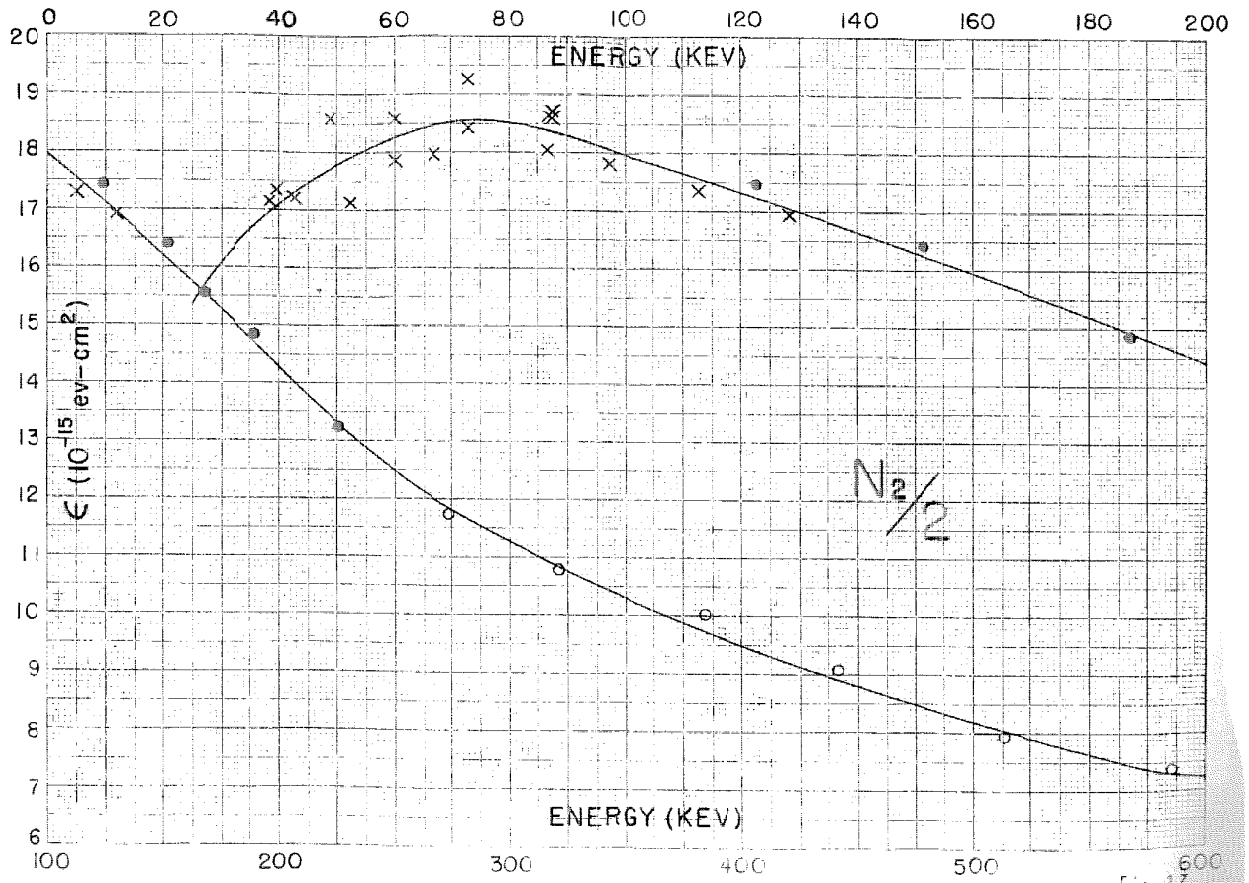
ENERGY (KEV)
ϵ (10^{-15} ev-cm^2)
$N_2/2$
ENERGY (KEV)
0
20
40
60
80
100
120
140
160
180
200
6
7
8
9
10
11
12
13
14
15
16
17
18
19
20
100
200
300
400
500
600

Fig. 17

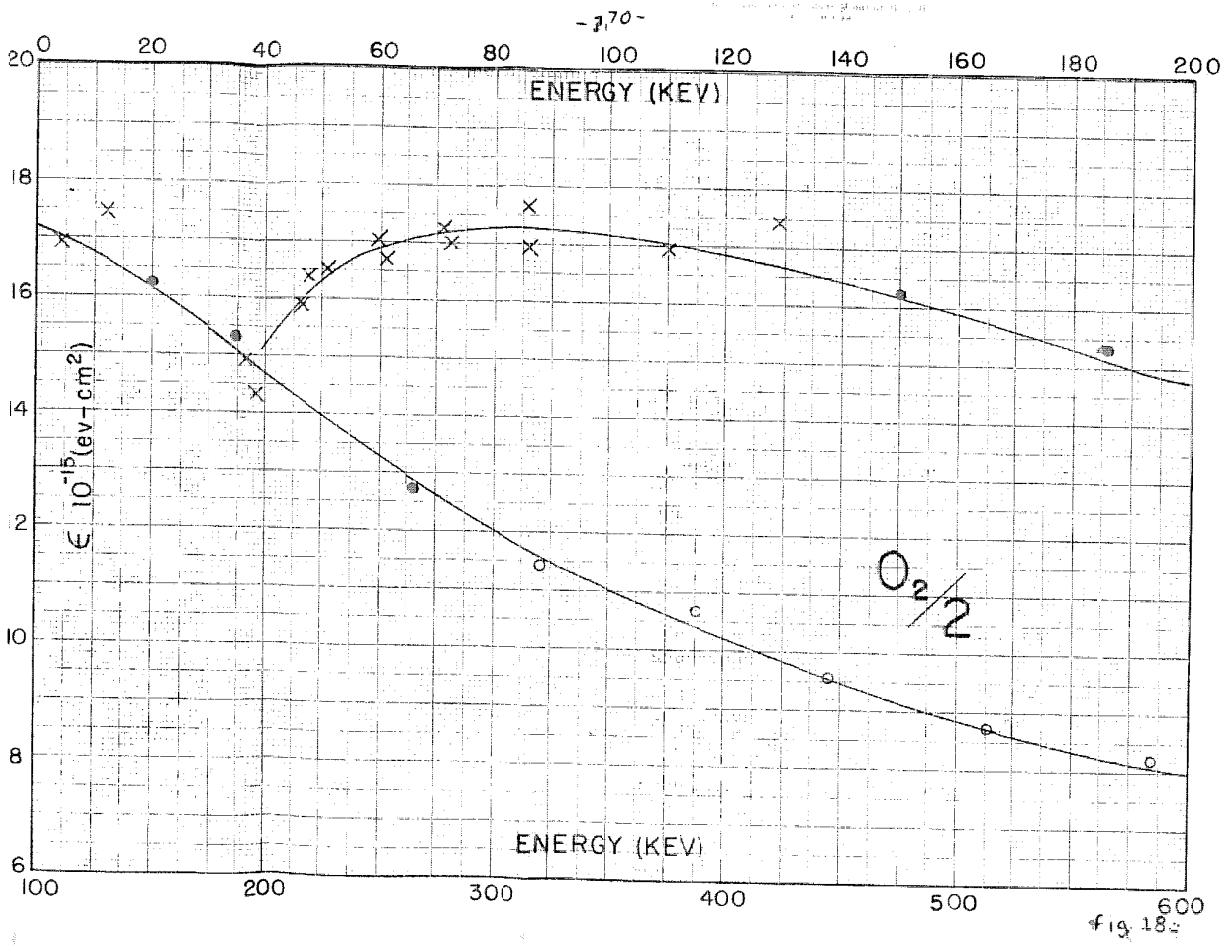
ENERGY (KEV)
ϵ 10^{-15}(ev-cm^2)
$O_2/2$
ENERGY (KEV)
0
20
40
60
80
100
120
140
160
180
200
18
16
14
2
10
8
6
100
200
300
400
500
600

Fig. 18

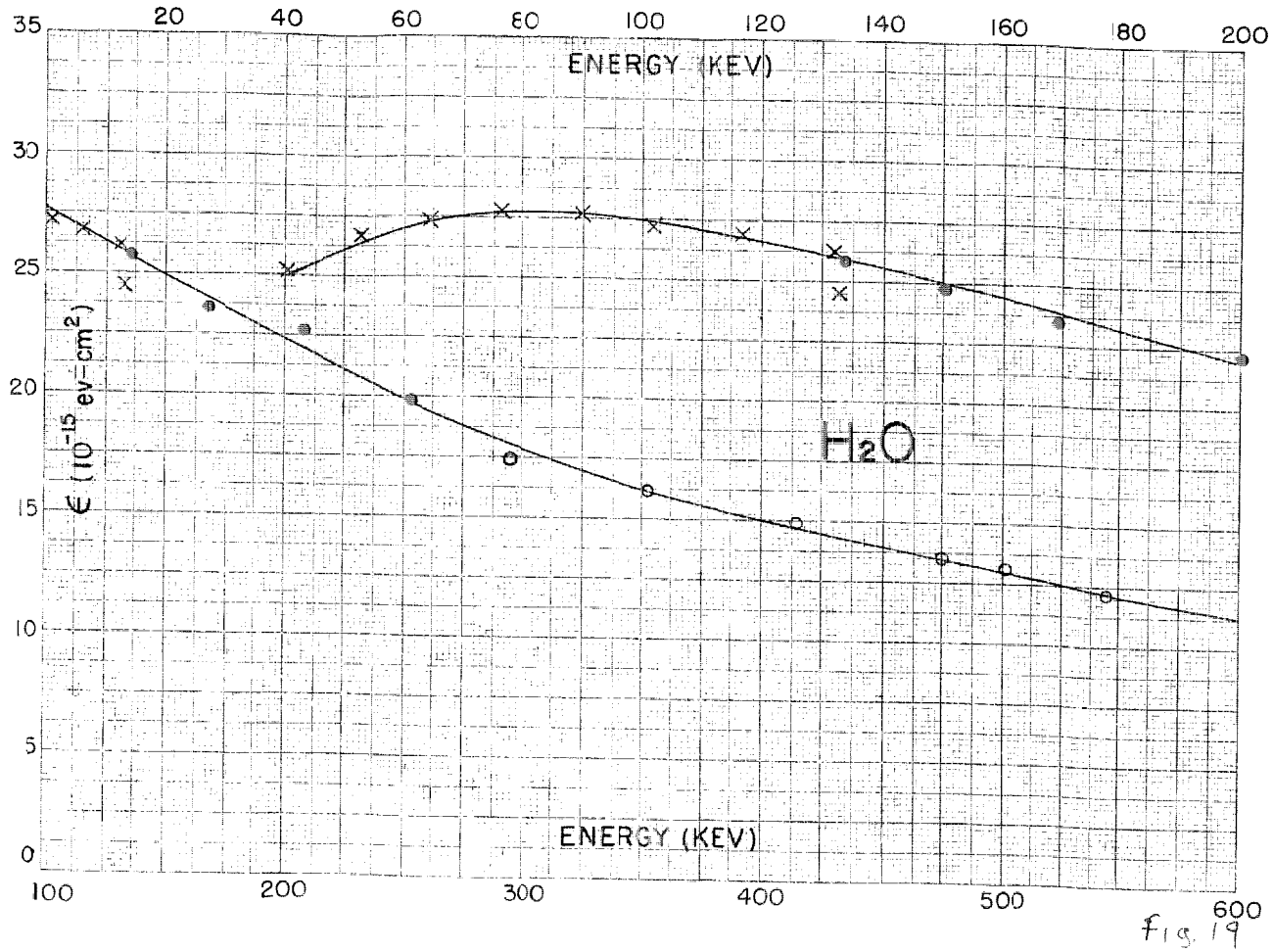
ENERGY (KEV)
H_2O
ϵ (10^{-15} ev-cm^2)
ENERGY (KEV)
0
5
10
15
20
25
30
35
20
40
60
80
100
120
140
160
180
200
100
200
300
400
500
600

Fig. 19

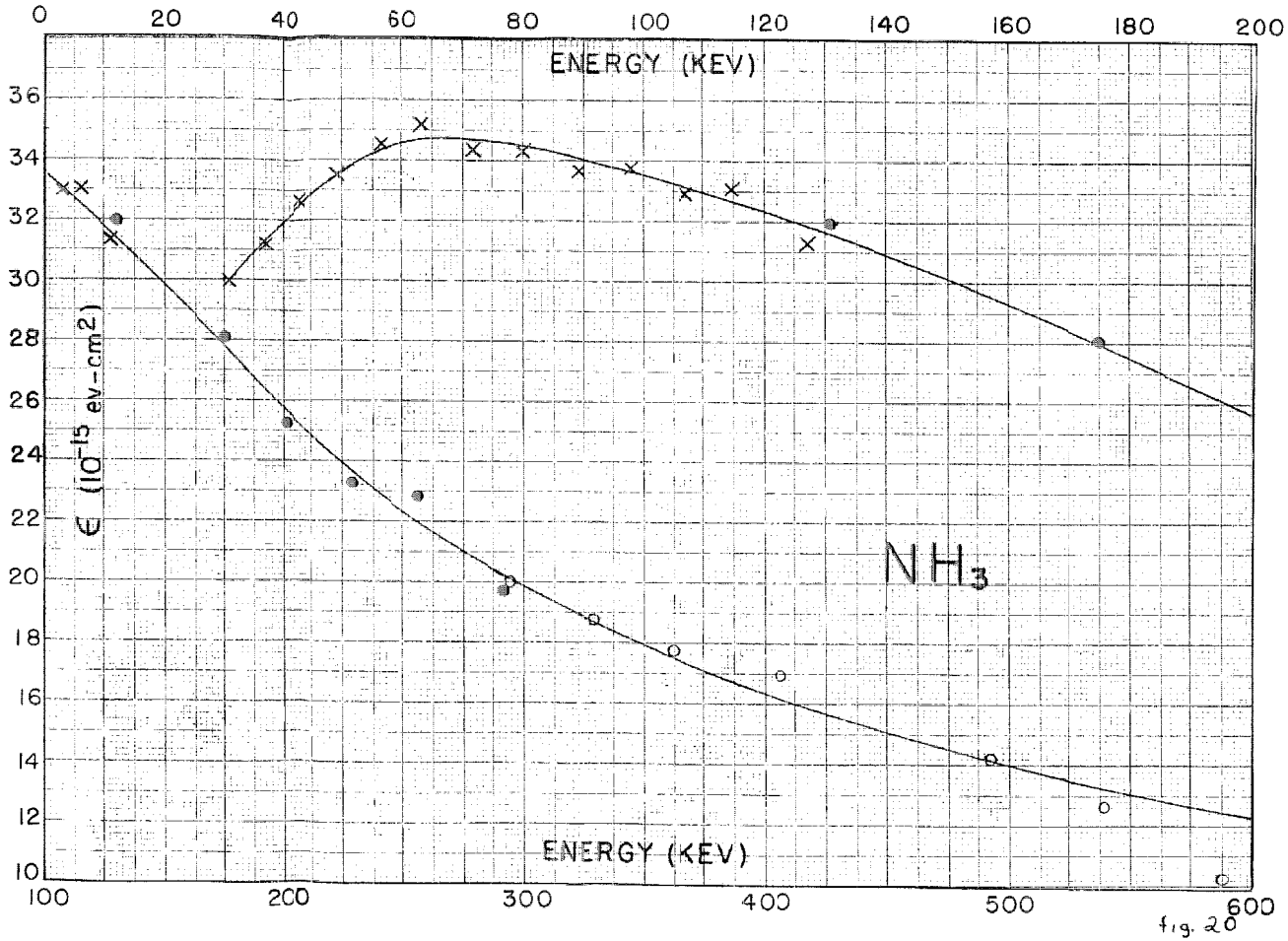
ENERGY (KEV)
ε (10⁻¹⁵ ev-cm²)
NH₃
ENERGY (KEV)
0
20
40
60
80
100
120
140
160
180
200
36
34
32
30
28
26
24
22
20
18
16
14
12
10
100
200
300
400
500
600

fig. 20

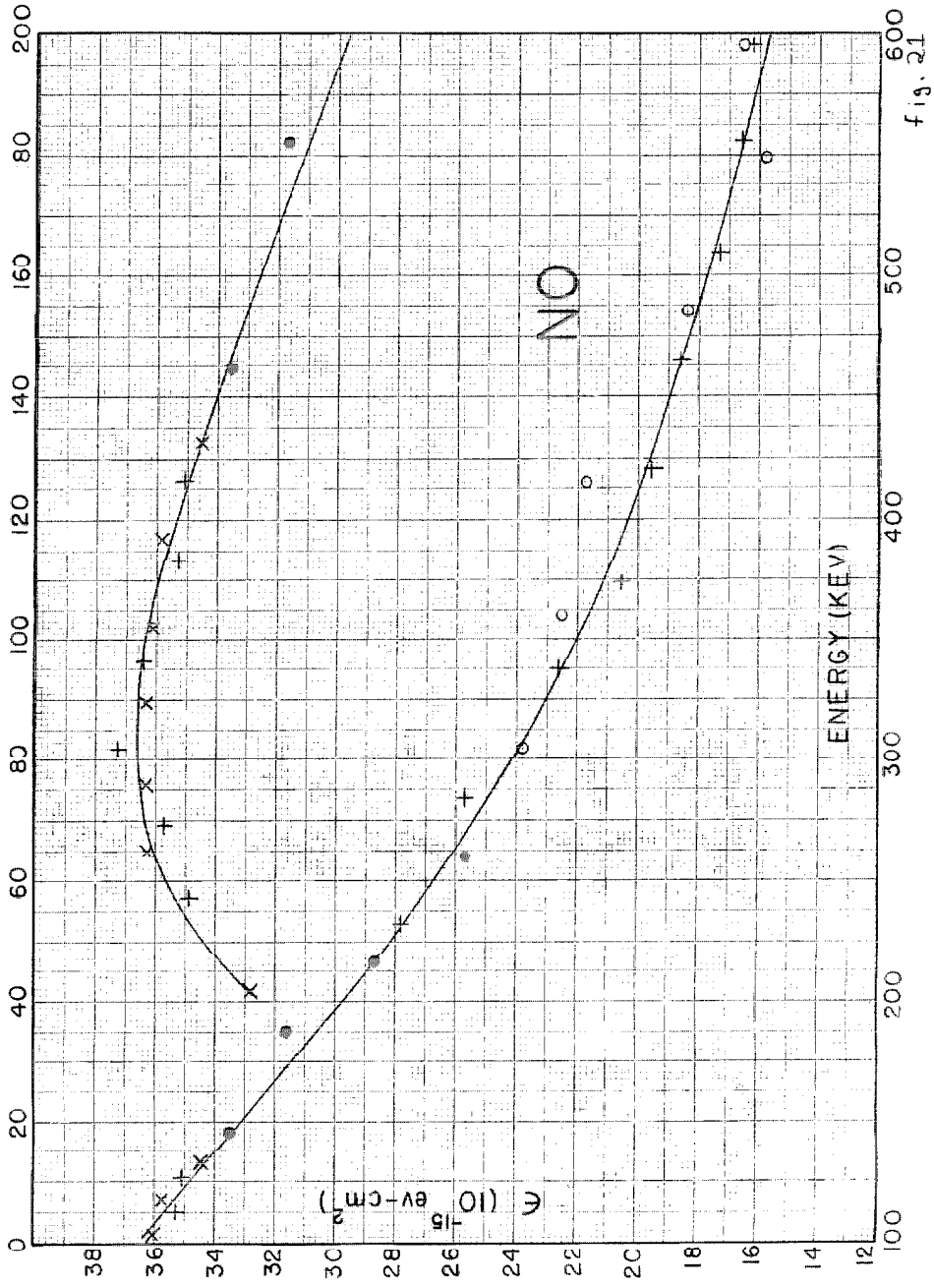

fig. 21

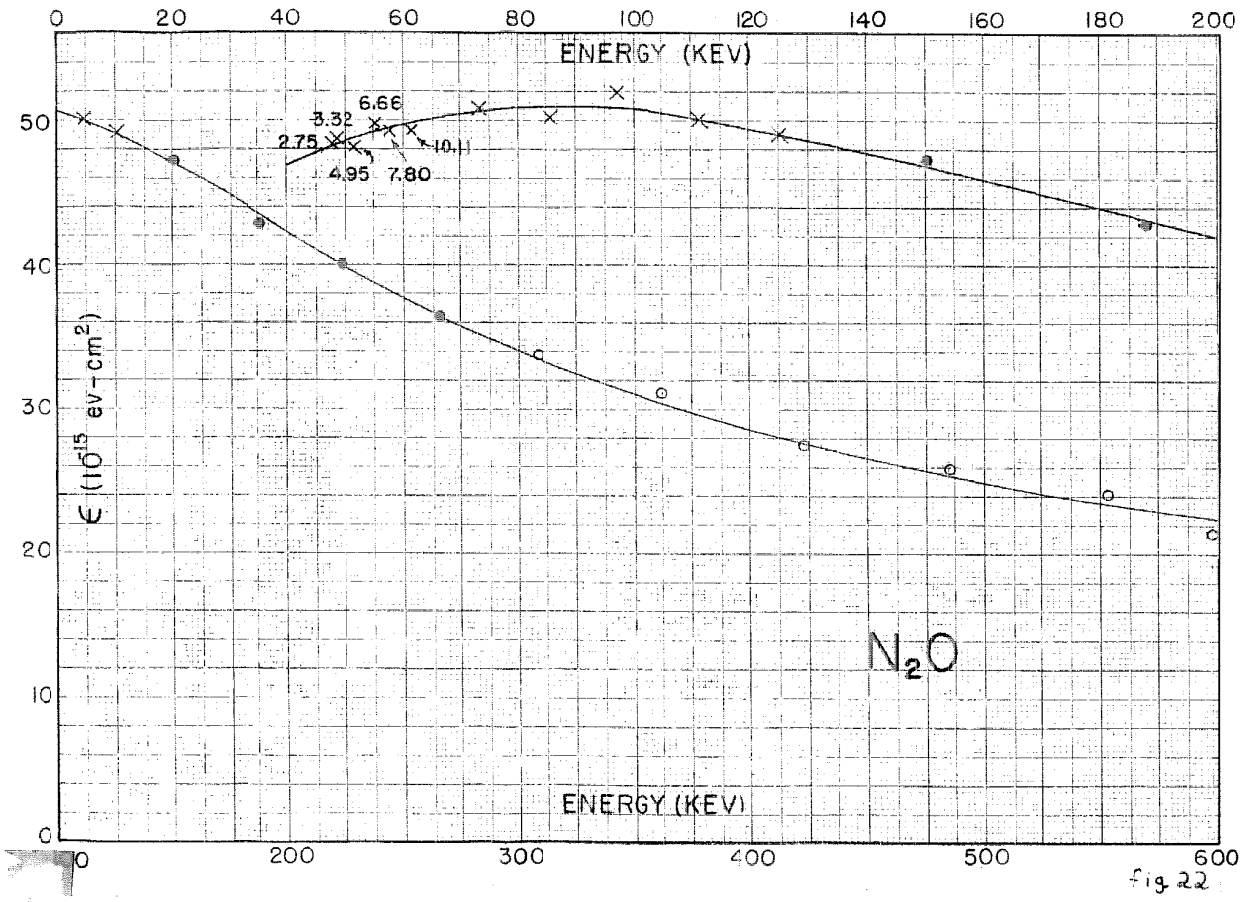
0
20
40
60
80
100
120
140
160
180
200
ENERGY (KEV)
6.66
3.32
2.75
4.95
7.80
10.11
50
40
30
20
10
0
ϵ (10^{15} ev-cm^2)
N_2O
ENERGY (KEV)
0
200
300
400
500
600

fig 22

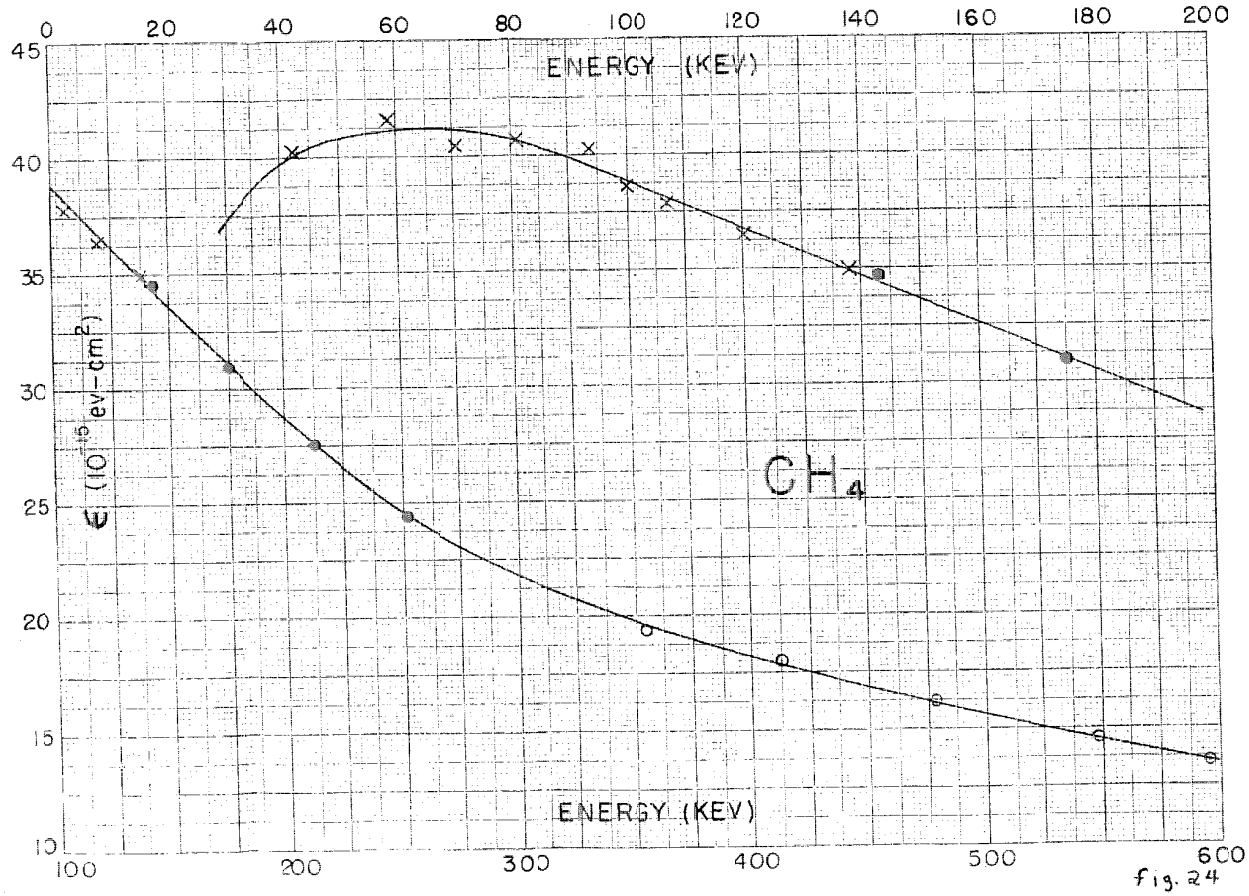
0
20
40
60
80
100
120
140
160
180
200
ENERGY (KEV)
45
40
35
30
25
20
15
10
ε (10^15 ev-cm^2)
CH4
100
200
300
400
500
600
ENERGY (KEV)

fig. 24

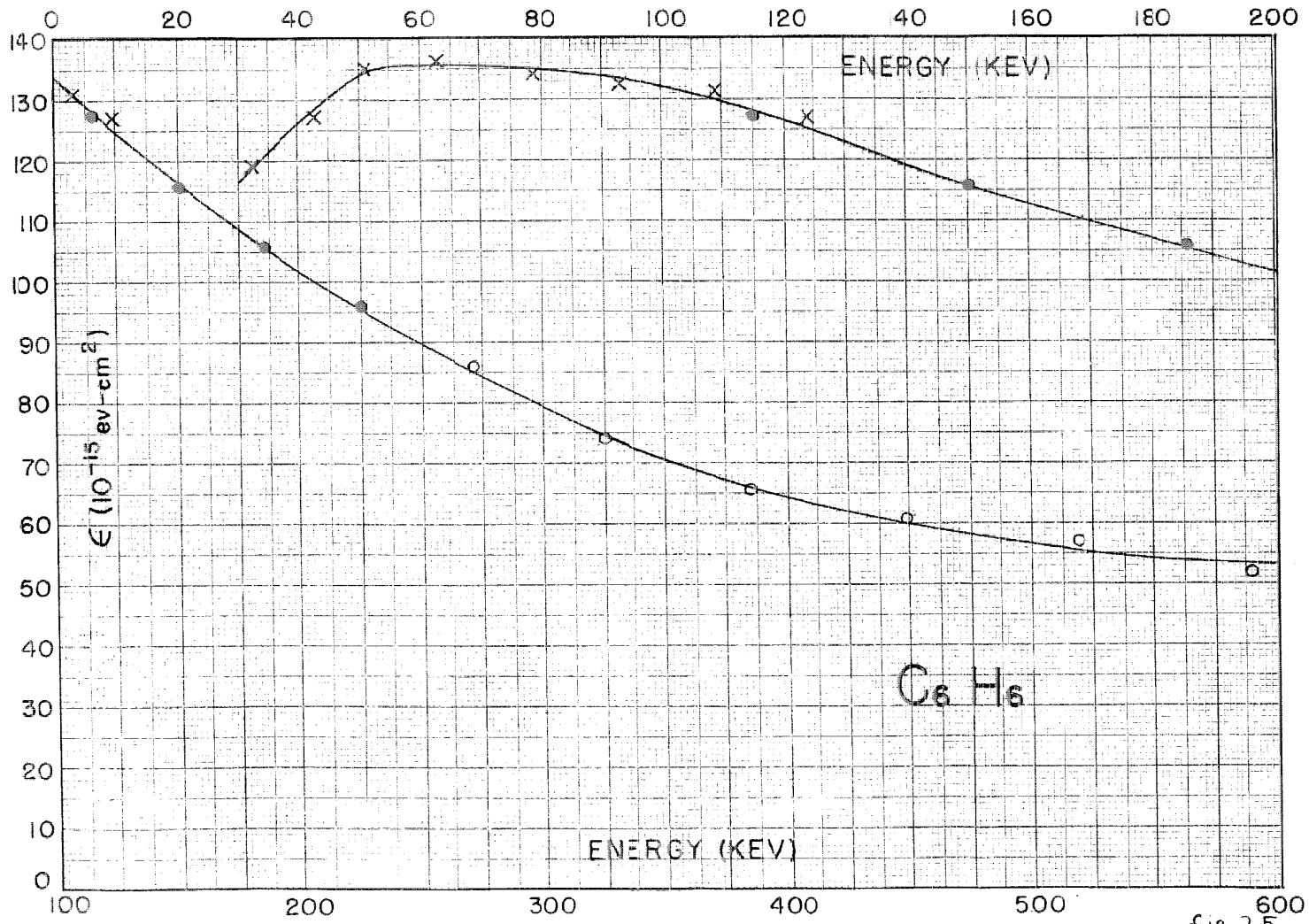
ENERGY (KEV)
ϵ (10^{-15} ev-cm^2)
$C_6 H_6$
ENERGY (KEV)
0
20
40
60
80
100
120
40
160
180
200
140
130
120
110
100
90
80
70
60
50
40
30
20
10
0
100
200
300
400
500
600

fig. 25

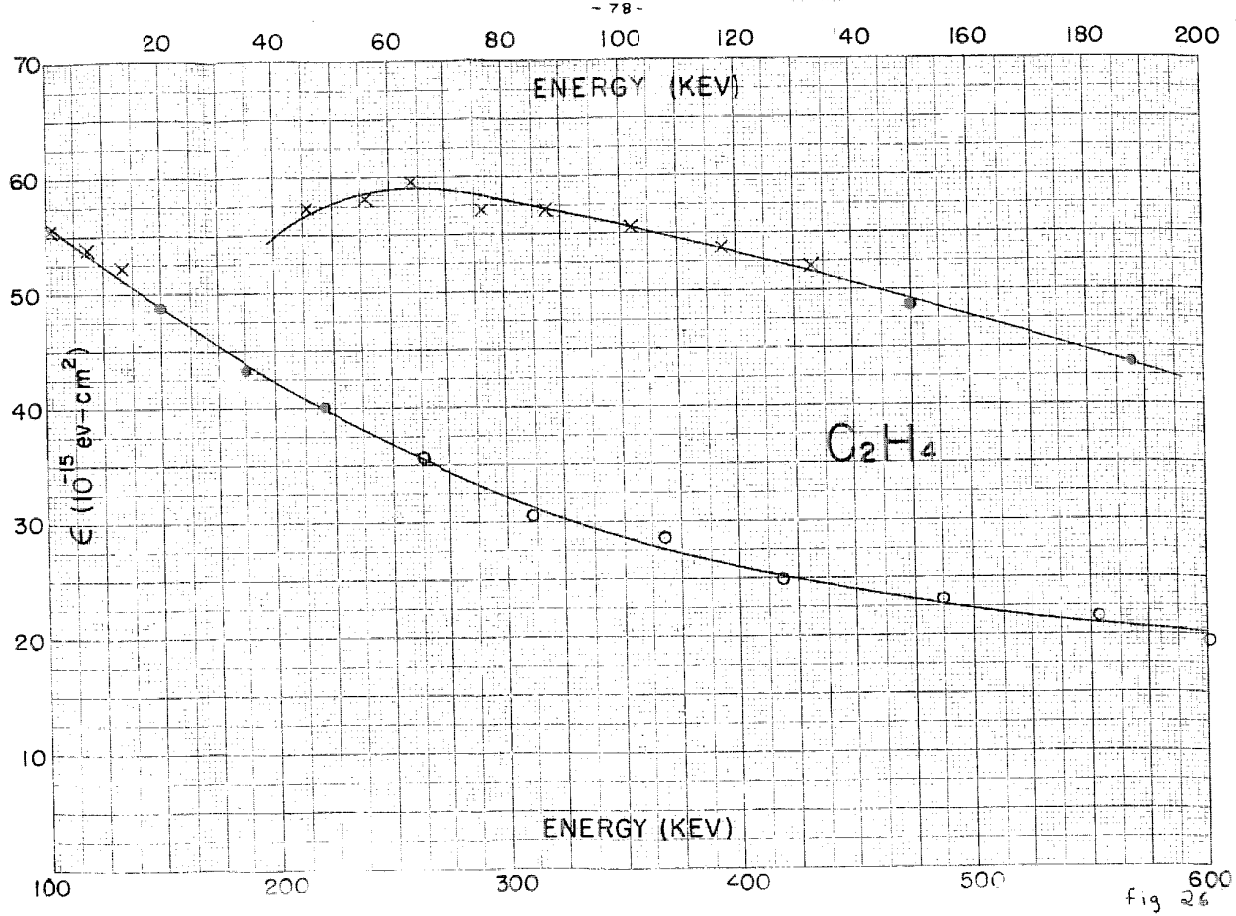
20
40
60
80
100
120
40
160
180
200
ENERGY (KEV)
70
60
50
40
30
20
10
ϵ (10^{-15} ev-cm^2)
C_2H_4
ENERGY (KEV)
100
200
300
400
500
600

fig 26

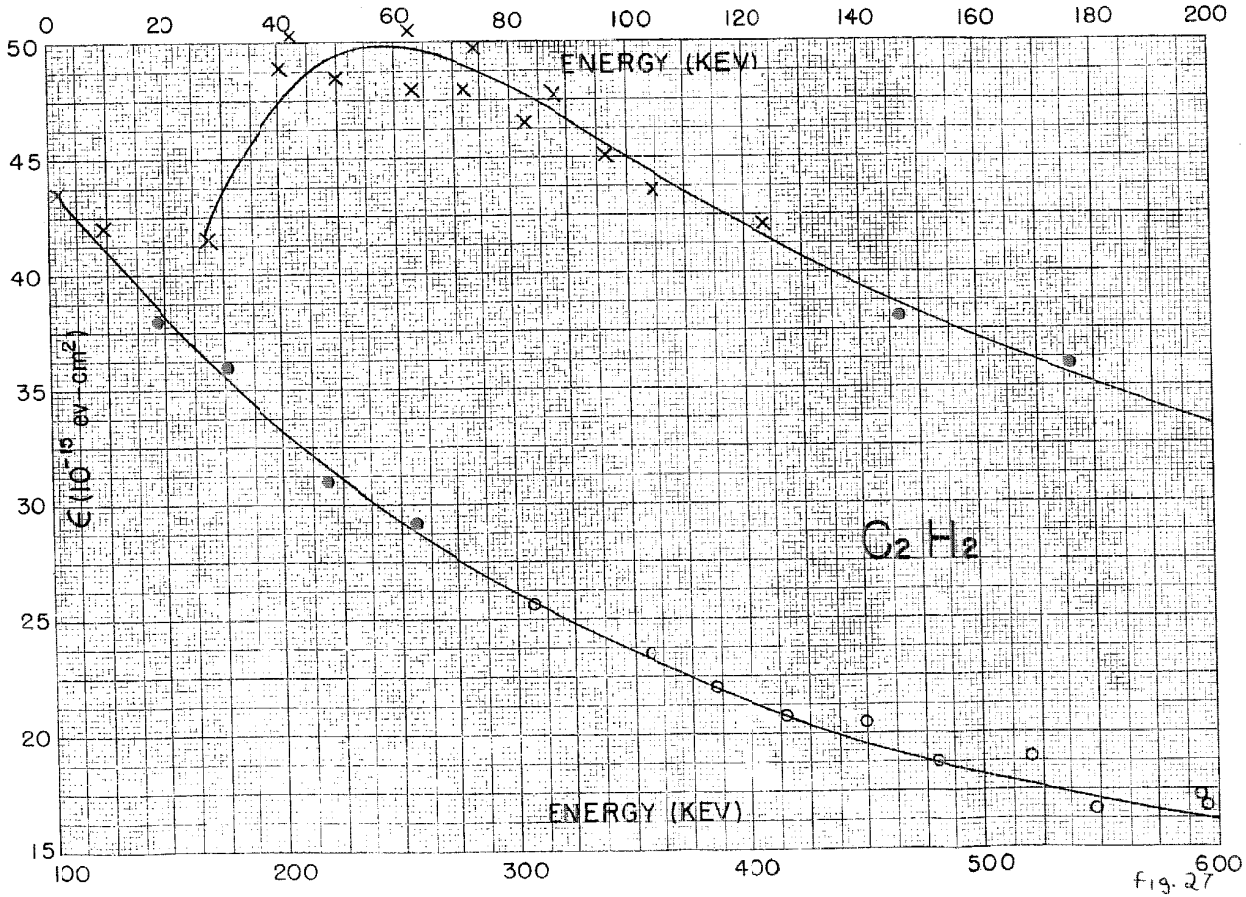
ENERGY (KEV)
C_2H_2
ENERGY (KEV)
ϵ (10^{-15} ev-cm^2)
0
20
40
60
80
100
120
140
160
180
200
50
45
40
35
30
25
20
15
100
200
300
400
500
600

Fig. 27

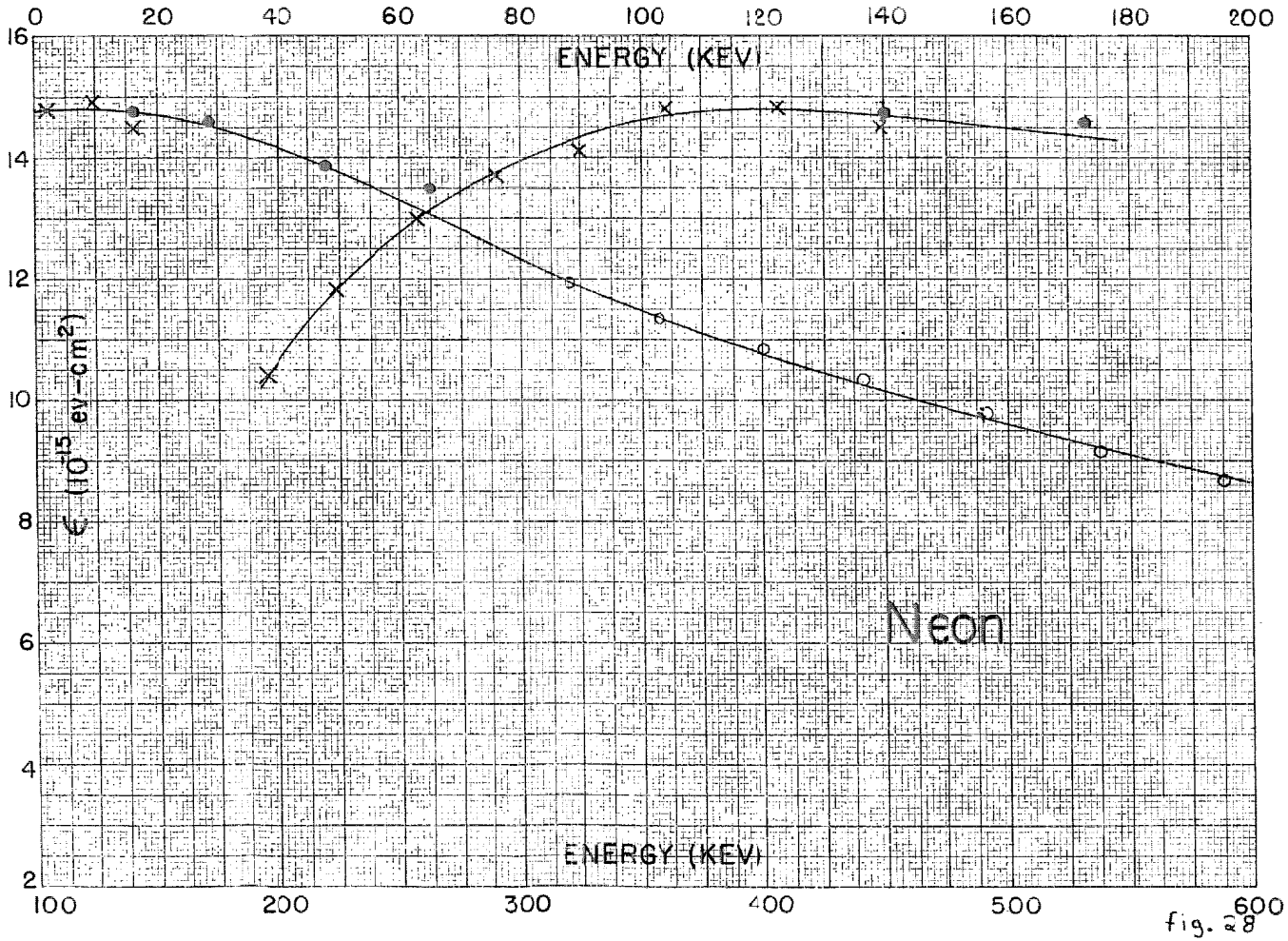
ENERGY (KEV)
ε (10⁻¹⁵ ev-cm²)
Neon
ENERGY (KEV)
0
20
40
60
80
100
120
140
160
180
200
2
4
6
8
10
12
14
16
100
200
300
400
500
600

fig. 28

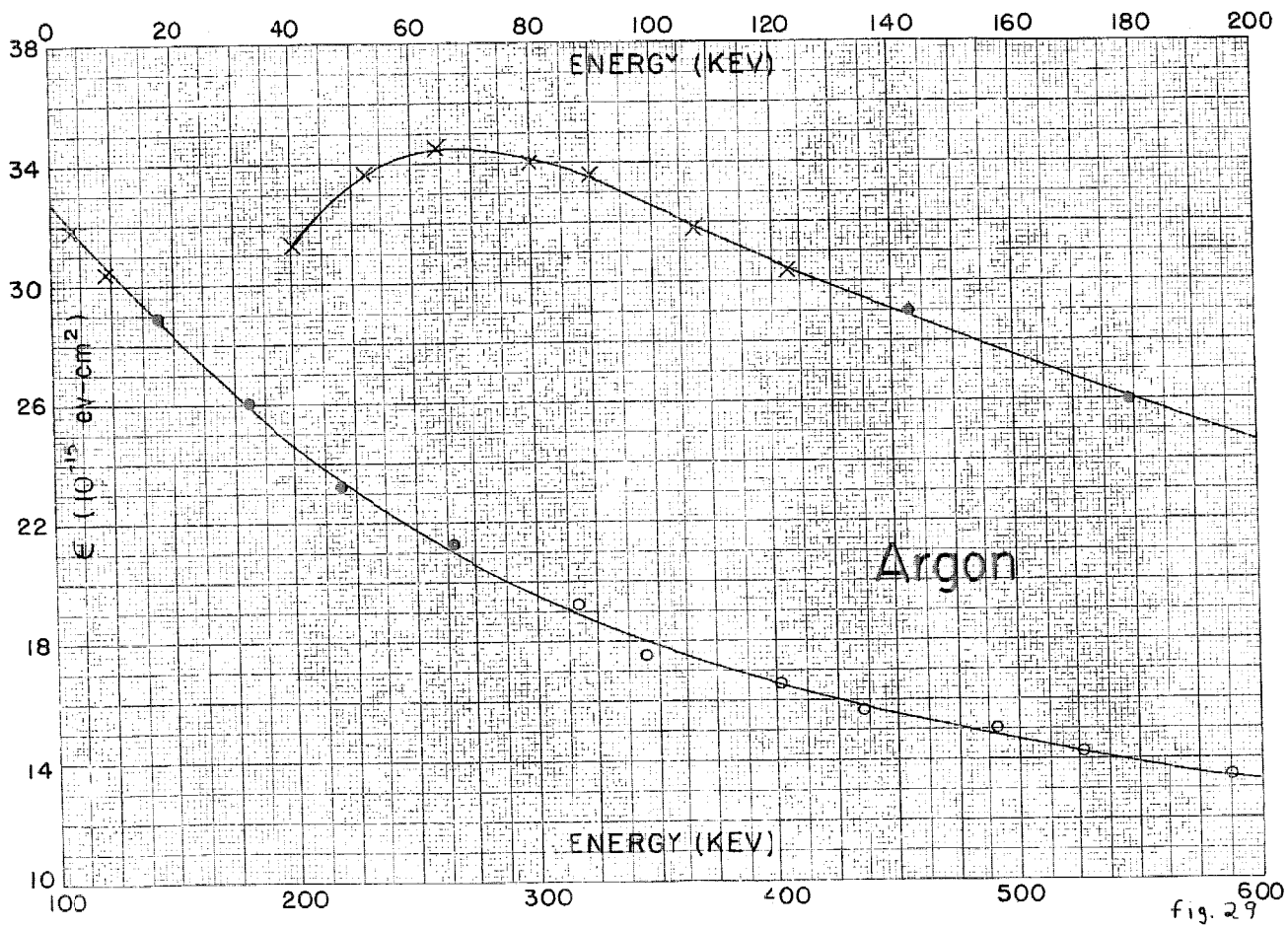
ENERGY (KEV)
Argon
ENERGY (KEV)
ε (10^15 ev-cm^2)
0
20
40
60
80
100
120
140
160
180
200
38
34
30
26
22
18
14
10
100
200
300
400
500
600

fig. 29

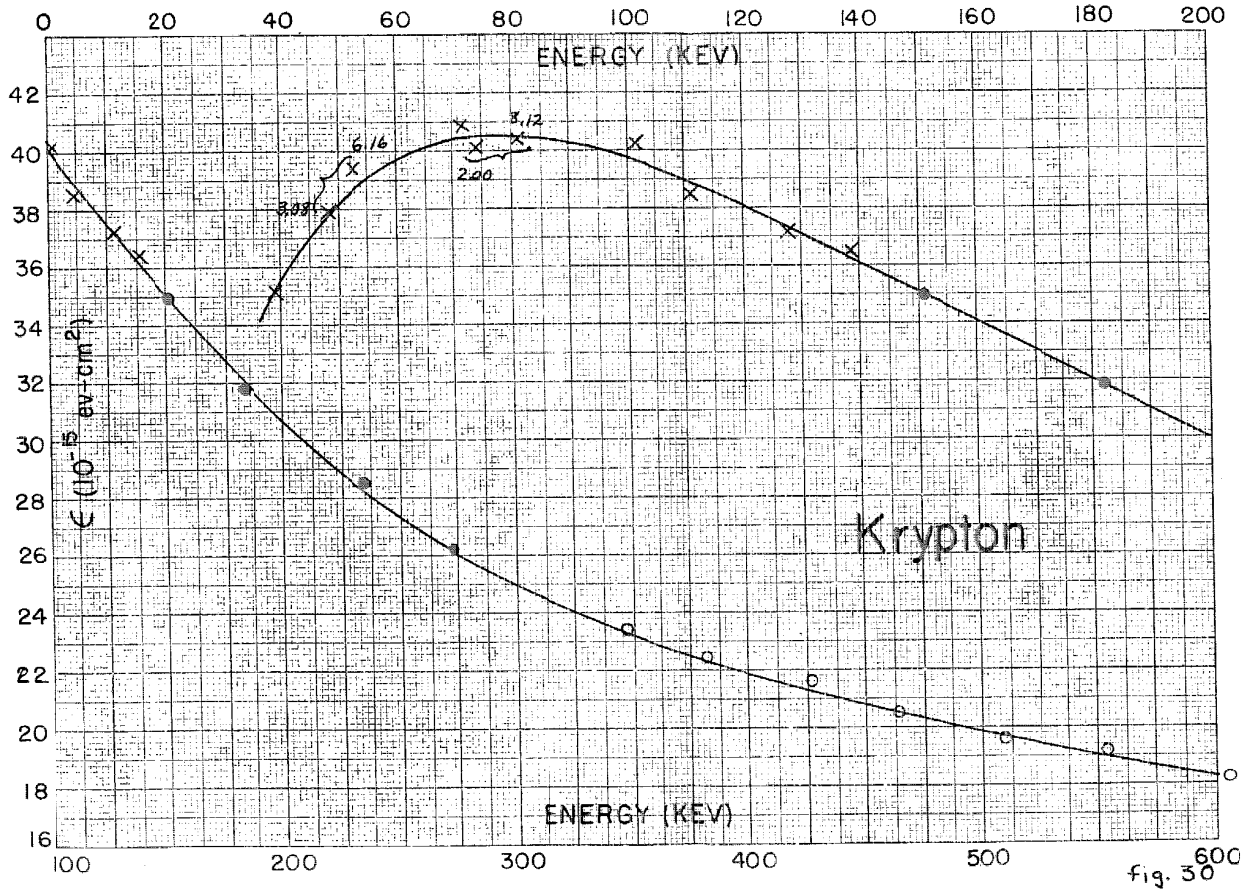
ENERGY (KEV)
Krypton
ENERGY (KEV)
ε (10⁻¹⁵ ev-cm²)
3.12
6.16
3.03
2.00
0
20
40
60
80
100
120
140
160
180
200
42
40
38
36
34
32
30
28
26
24
22
20
18
16
100
200
300
400
500
600

fig. 30

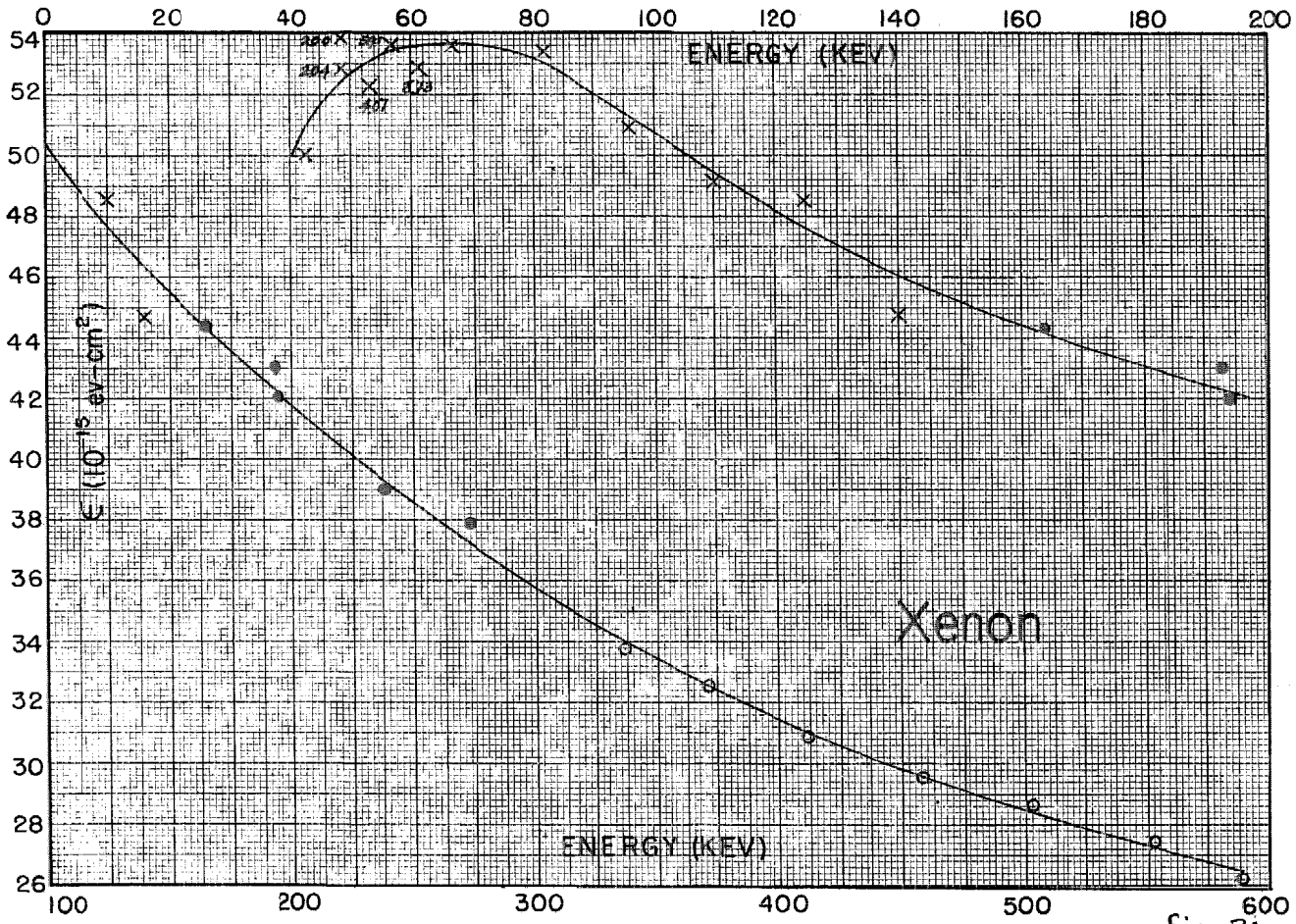
ENERGY (KEV)
ENERGY (KEV)
Xenon
W (1-5 eV-cm²)
0
20
40
60
80
100
120
140
160
180
200
54
52
50
48
46
44
42
40
38
36
34
32
30
28
26
100
200
300
400
500
600

fig. 31

REFERENCES

(1) Snyder, C. W., S. Rubin, W. A. Fowler, C. C. Lauritsen, Rev. Sci. Inst. 21, 852 (1950).

(2) Wenzel, W. A., and W. Whaling, Phys. Rev. 87, 499 (1952).

(3) Platzman, R. L., "Symposium on Radiobiology," John Wiley & Son, New York, p. 139 (1952).

(4) Gray, L. H., Proc. Camb. Phil. Soc. 40, 72 (1944).

(5) Kramers, H. A., Physica, 13, 401 (1947).

(6) Michl, W., Sitzber Akad. Wiss. Math.-naturw. Kl. Abt. IIA, 123, 1965 (1914).

(7) Phillip, K., Zeit. Physik, 17, 23 (1923).

(8) Appleyard, R. K., Nature, 163, 526 (1949).

(9) de Carvalho, H. G., and H. Yagoda, Phys. Rev. 88, 273 (1952).

(10) Crenshaw, C. M., Phys. Rev. 62, 54 (1942).

(11) Bethe, H. A., Rev. Mod. Phys. 22, 213 (1950).

(12) Kanner, H., Phys. Rev. 84, 1211 (1951).

(13) Montague, J. H., Phys. Rev. 81, 1026 (1951).

(14) Ribe, F. L., Phys. Rev. 83, 1217 (1951).

(15) Warshaw, S. D., Phys. Rev. 76, 1763 (1949).

(16) Allison, S. K., (private communication).

(17) Bethe, H. A., Ann. de Physik, 5, 325 (1930).

(18) Livingston, M. S. and H. A. Bethe, Rev. Mod. Phys. 9, 245 (1937).

(19) Brown, L. M., Phys. Rev. 79, 297 (1950).

(20) Walske, M. C., Phys. Rev. 88, 1283 (1952).

(21) Wenzel, W. A., Thesis, California Institute of Technology (1952).

(22) Li, C. W., Thesis, California Institute of Technology (1951).

(23) Sawyer, G. A., Rev. Sci, Inst. 23, 604 (1952).

(24) Mather, R. and E. Segre', Phys. Rev. 84, 191 (1951).

(25) Schmieder, K., Ann. de Physik, 35, 445 (1939).

(26) Bøggild, J. K., Det. Kgl. Dan. Vid. Selsk. 23, No. 4 (1945).

(27) Hughes, D. J. and C. Eggeler, Phys. Rev. 75, 782 (1949).

(28) Chilton, A. and J. N. Cooper, (private communication).

(29) Weyl, P. K. and S. K. Allison, (private communication).

(30) Phillips, J. A., (to be published, private communication).

(31) Moorish, A. H., Phys. Rev. 76, 1651 (1949).

(32) Bohr, N., Det. Kgl. Dan.Vid. Selsk. 18, No. 8 (1949).